Transfer and neutron capture reactions to ^{194}Ir as a test of $U_\nu(6/12)\otimes U_\pi(6/4)$ supersymmetry

M. Balodis,[1] H.-F. Wirth,[2,3,*] G. Graw,[2] R. Hertenberger,[2] J. Bērziņš,[1] N. Krāmere,[1] J. Jolie,[4] S. Christen,[4] O. Möller,[4] D. Tonev,[4] J. Barea,[5] R. Bijker,[5] A. Frank,[5] and T. von Egidy[3]

[1]*Institute of Solid State Physics, University of Latvia, Riga, LV-1063, Latvia*

[2]*Department für Physik, Ludwig-Maximilians-Universität München, D-85748 Garching, Germany*

[3]*Physik-Department, Technische Universität München, D-85748 Garching, Germany*

[4]*Institut für Kernphysik, Universität zu Köln, D-50937 Köln, Germany*

[5]*Instituto de Ciencas Nucleares, Universidad Nacional Autónoma de México, AP 70-543, 04510 Mexico DF, Mexico*

(Received 25 July 2007; revised manuscript received 28 March 2008; published 5 June 2008)

The structure of ^{194}Ir is investigated via (n,γ), (n,e^-), (d,p), and $(\vec{d},\alpha)$ spectroscopy. The use of different methods leads to an almost complete level scheme up to high excitation energies including γ-decay and spin-parity assignments. A reanalysis of the formerly published (n,γ) data was triggered by our new (d,p) and $(\vec{d},\alpha)$ transfer reactions. The experimental level scheme is compared to predictions using extended supersymmetry. Herein, the classification of states was done according to quantum numbers, excitation energies, and $(\vec{d},\alpha)$ transfer strengths. A one-to-one correspondence in excitation energies was obtained for the 23 lowest lying theoretical states with similar structures for the experimental and calculated level schemes. The two-nucleon transfer strengths show remarkable agreement. A Nilsson classification is discussed as well.

DOI: 10.1103/PhysRevC.77.064602 PACS number(s): 21.10.Jx, 23.20.Lv, 21.60.Ev, 27.80.+w

I. INTRODUCTION

The odd-odd nucleus ^{194}Ir belongs to the most interesting and complicated heavy nuclei, because it lies in the transitional region where the shape of the nuclei is not well defined. A well-known level scheme would allow one to test both geometrical and algebraic nuclear models. It was shown earlier [1] that the low-energy levels can be partially understood as rotational bands on Nilsson orbits. Triaxial shape models can be used for the interpretation of the level scheme. Besides, tests of the interacting boson fermion-fermion model (IBFFM) as well as the supersymmetry (SUSY) approach are of particular interest.

Two publications [1,2] of the previous decade and the Nuclear Data Sheets [3] provide information on previous experimental studies. A theoretical description using the IBFFM model and the extended SUSY $U_\nu(6/12)\otimes U_\pi(6/4)$ is given in Ref. [4].

In the present work, a more detailed knowledge of the ^{194}Ir level structure is achieved than that in publication [1]. It has been enabled by new experimental results from the (d,p) and $(\vec{d},\alpha)$ reactions and by the more complete evaluation of the earlier measured (n,γ) and (n,e^-) spectra after thermal neutron capture. The $(\vec{d},\alpha)$ measurement partially reported in the NDS [3] based on an annual report is published in detail here for the first time.

We compare new extended supersymmetry $U_\nu(6/12)\otimes U_\pi(6/4)$ calculations with our data. Of special interest is the new comparison with predictions of transfer strengths [5] for the $(\vec{d},\alpha)$ reactions.

Our work is structured as follows: Section II describes the experiments performed. In Sec. III we discuss the new level scheme. Section IV compares the data to theory using a Nilsson classification and then the extended supersymmetry approach. Finally, Sec. V gives our conclusions.

II. EXPERIMENTAL DATA

A. Transfer reactions

The excitation spectrum of ^{194}Ir was studied in (d,p) and polarized $(\vec{d},\alpha)$ transfer experiments at the tandem Van de Graaff accelerator [6] and the Q3D magnetic spectrograph [7] of the accelerator laboratory (Maier-Leibnitz-Labor) of Ludwig-Maximilians-Universität and Technische Universität München. Both experiments provide specific information: a rather complete set of excitation energies is obtained from the ^{193}Ir$(d,p)^{194}$Ir spectra which have an energy resolution of about 5 keV, while the ^{196}Pt$(\vec{d},\alpha)^{194}$Ir transfer reaction from a $J^\pi = 0^+$ target provides unique J^π assignments.

The outgoing protons and α particles were momentum separated by the Q3D magnetic spectrograph with a solid angle acceptance of 11 msr. The focal plane detector is a position-sensitive proportional counter with single-strip readout of a cathode foil and $\Delta E/E_{\mathrm{rest}}$ particle identification [8,9]. The integration of the beam current in a Faraday cup allowed the determination of absolute cross sections. The polarized deuteron beam was provided by the Stern-Gerlach source [10] with adiabatic high-frequency transitions. The orientation of the vector polarization [$P_y = 65(\pm5)\%$] of the beam was interchanged without effect on the beam position at the target. The polarized deuteron current on target was up to 2 μA.

1. ^{193}Ir$(d,p)^{194}$Ir measurement

Proton spectra of the reaction ^{193}Ir$(d,p)^{194}$Ir were recorded at the three angles 20°, 40°, and 60°. The target consisted of 130 μg/cm^2 enriched ^{193}Ir (99%) evaporated on a 5 μg/cm^2

*Corresponding author. wirth@tum.de

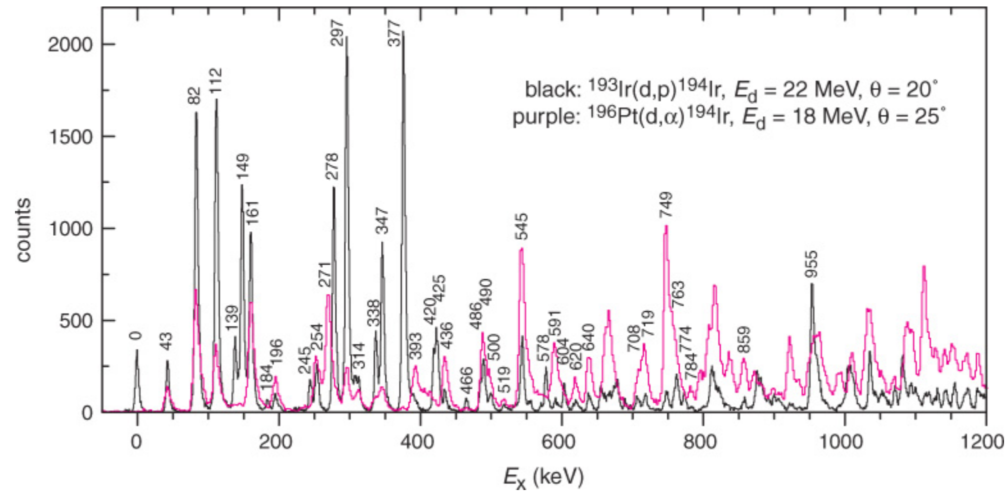

FIG. 1. (Color online) Energy calibrated spectra of the ^{193}Ir$(d,\ p)^{194}$Ir reaction at $E_d = 22$ MeV and $\theta = 20^\circ$ (black) and the ^{196}Pt$(d,\alpha)^{194}$Ir reaction at $E_d = 18$ MeV and $\theta = 25^\circ$ (purple). Some peaks are labeled with their energy in keV. Most of the excited levels are observed in both reactions, cf. Table I, whereas the ground state is nearly not visible in (d,α).

carbon backing. The energy of the incoming deuteron beam was 22 MeV. The 20° spectrum is shown in Fig. 1 in black. The energy resolution is 5–6 keV full width at half maximum (FWHM). In Fig. 1, the $(d,\alpha)^{194}$Ir spectrum at 25° (sum of spin up and spin down spectra) is superimposed to demonstrate the different population of some levels in both reactions; see, for example, the ground state and the 271 keV state. The three measured $(d,\ p)$ spectra were used to average the peak energies and to reduce statistical effects. The energy calibration was done using well-known energies from Ref. [1] and the new (n,γ) evaluation reported in this paper. The observed levels and their cross section at 20° are listed in Table I. A total of 62 levels have been observed up to 963 keV. Since the level density increases rapidly (see Fig. 1) we restricted the evaluation to this excitation energy. As one can see from Table I, the last point used for the energy calibration of this $(d,\ p)$ measurement was the 708.5 keV level. The deviation of a few keV at 1 MeV excitation energy compared to the former $(d,\ p)$ measurement [11] can result from the extrapolation of the energy calibration.

The analysis of the $(d,\ p)$ angular distributions is in many cases ambiguous. Up to four transferred angular momenta couple to the 3/2 ground state spin of the target nucleus ^{193}Ir and add incoherently to the same final state in ^{194}Ir. To get information on the spin and parity of states in ^{194}Ir, we measured the ^{196}Pt$(\vec{d},\alpha)^{194}$Ir reaction. The levels obtained from $(d,\ p)$ are essential for evaluating $(\vec{d},\alpha)$ and to develop the level scheme from (n,γ), since many doublets unresolved in the former $(d,\ p)$ measurement (e.g., the 192.7 keV peak) are now resolved.

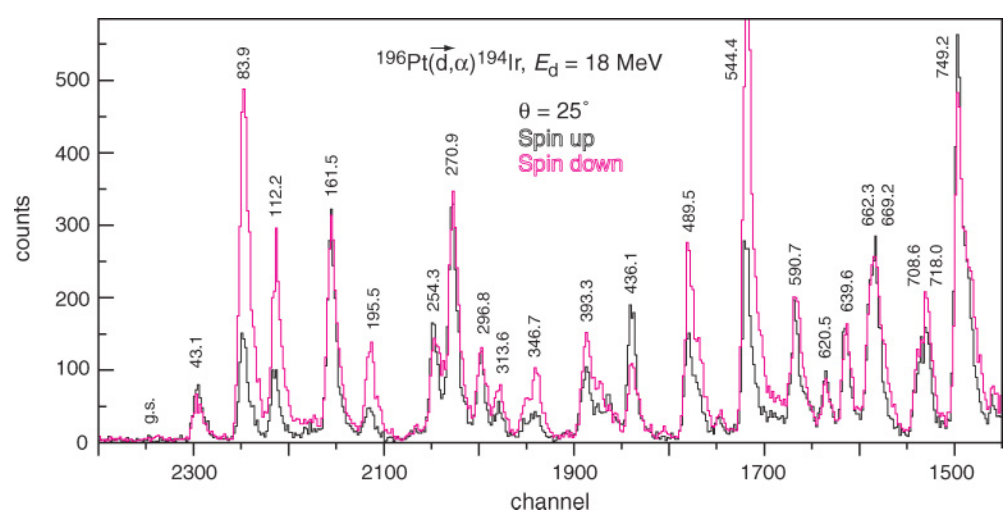

FIG. 2. (Color online) Spin up and spin down spectra of the ^{196}Pt$(\vec{d},\alpha)^{194}$Ir reaction at $E_d = 18$ MeV and $\theta = 25^\circ$. Some peaks are labeled in keV. One sees the big effect of the change of the deuteron beam polarization on the individual strengths which leads to a valuable analyzing power, cf. Figs. 3 and 6.

TABLE I. Levels observed in the ^{193}Ir$(d, p)^{194}$Ir and the ^{196}Pt$(\vec{d}, \alpha)^{194}$Ir reaction. The energies are averaged over the three and nine measured angles, respectively. The ^{194}Ir excitation levels compiled in the NDS [3] are given up to 600 keV. The energies of (n, γ) and a former (d, p) measurement are given, too. The energy calibrations of the (d, p) measurements differ up to 7 keV at 1 MeV (cf. text). For the $(\vec{d}, \alpha)$ reaction, the proposed J^{π} value is given compared with values from the NDS [3] and Ref. [1]. For both reactions, the absolute cross sections at 20° are given. The last two columns give the spectroscopic strengths of the transfers in $(\vec{d}, \alpha)$.

E_x(keV)					J^{π}			$(d\sigma/d\Omega)^{20^\circ}$ (μb/sr)		$G_{\mathrm{LJ}}^{(1)}(10^{-3})$	$G_{\mathrm{LJ}}^{(2)}(10^{-3})$
NDS [3]	(n, γ) [1][a]	(d, p) [11]	(d, p)	$(\vec{d}, \alpha)$	NDS [3]	Ref. [1]	$(\vec{d}, \alpha)$	(d, p)	$(\vec{d}, \alpha)$	$(\vec{d}, \alpha)$	$(\vec{d}, \alpha)$
0.0	0.0[b]	0.10(16)	0.0	0.0	1^-	1^-	(1^-)	30	0.1	1.2	–
43.119(1)	43.119(1)[b]	43.06(16)	43.2(3)	43.1(3)	0^-	0^-	0^-	24	1.5	7.2	–
82.336(1)	82.336(1)				1^-	1^-					
84.285(1)	84.285(1)	83.88(8)	84.0(3)	83.9(3)	2^-	2^-	2^-	162	5.4	1.8	9.6
112.232(1)	112.231(1)[b]	112.22(8)	112.3(3)	112.2(3)	2^-	2^-	2^-	173	2.7	3.3	4.2
138.688(1)	138.688(1)[b]	138.4(4)	138.7(3)	138.5(5)	1^-	1^-	$(0^-, 1^-)$	37	0.3	1.4, 2.2	–, –
143.592(1)	143.592(1)				0^-	0^-					
147.072(2)	147.074(1)				4^+	4^+					
148.934(1)	148.935(1)[b]	148.75(13)	148.8(3)	148.2(7)	$(2, 3)^-$	3^-	$2^-, (3^-)$	115	0.3	0.6, 0.8	0.4, –
160.998(1)	160.998(1)[b]	161.14(13)	161.0(3)		1^-	1^-		92			
161.5	*161.518(2)*[c]			161.5(3)	(5^+)	5^+[c]	$5^+, (4^-)$		6.0	22.3, 7.0	9.6, 12.1
184.688(2)	184.688(2)		184.0(3)		3^-	3^-		6			
190.0+x					(10, 11)						
192.7 (10)											
195.527(1)	195.527(1)	192.7(10)	195.6(4)	195.5(3)	2^-	2^-	2^-	9	1.7	0.9	2.6
				235.8(6)					0.3		
245.110(1)	245.111(1)	244.4(4)	245.0(3)		$(3)^-$	3^-		15			
245.492?(2)	245.492(2)				(0^-)	0^-					
254.161(1)	254.161(1)[b]	255.1(3)	254.1(3)	254.3(3)	2–	2^-	2^-	22	2.1	11.0	0.0
270.917(2)	270.918(2)			270.9(3)	$(3, 4)^+$	$3, 4^+$	$(2^-, 3^+)$		4.2	12.8, 6.3	3.1, 14.7
278.505(2)	278.505(2)[b]	278.74(12)	278.5(3)		(2)–	2^-		107			
296.630(2)	296.631(2)[b]	296.34(10)	296.6(3)	296.8(3)	4^-	4^-	4^-	181	1.9	0.9	11.7
308.974(1)	308.974(1)	311.6(4)	308.1(4)		1^-	1^-		14			
314.053(2)	314.053(2)		313.8(4)	313.6(3)	2^-	2^-	2^-	13	0.7	2.6	0.5
337.524(2)	337.523(2)	337.4(4)	337.8(3)		1^-	1^-		36			
337.648(2)	337.649(2)			336.7(5)	2^-	2^-	2^-		0.7	0.5	0.8
347.051(2)	347.050(2)[b]	346.76(11)	347.1(3)	346.7(4)	3^-	3^-	$(2^-, 3^-)$	78	1.2	1.0, 2.6	1.5, –
371.282?(2)	371.277(7)				(3^-)	3^-					
				374.8(6)			$(4^-, 5^+)$		0.3	0.4, 1.1	0.0, 0.0
376.998(2)	377.009(3)[b]	376.76(11)	377.0(3)			3^-		179			
390.963(2)	390.963(2)	393.0(12)	388.0(9)			$1, 2, 3^-$		7			
	394.880(3)[c]		394.2(3)	393.3(3)		4^-[c]	$3^+, 4^-$	4	1.9	0.6, 0.4	10.3, 13.0
407.018?(3)	407.019(3)			406.4(5)	(3^+)	$(3)^+$	3^+		0.8	0.0	4.1
413.059?(5)	413.035(3)				(3^+)	$(3)^+$					
	416.590(5)[c]			416.0(6)		4^-[c]	(4^-)		0.9	1.1	0.7
419.611(3)	419.611(3)		419.9(3)		(3^-)	3^-		27			
423.727(2)	423.727(2)	422.15(15)	424.8(3)		2^-	2^-		30			
436.296(2)	436.296(2)	433.9(4)	435.6(3)	436.1(3)	2^-	2^-	2^-	8	1.9	8.3	0.3
467.208(3)	467.296(3)	467.7(4)	465.7(3)	466.9(8)	$(2, 3, 4)^-$	$2, 3, 4^-$		5	0.2		
	486.067(3)[d]		486.1(3)			2^-[d]		11			
489.649(3)	489.649(3)	489.55(18)	490.6(3)	489.5(3)	2^-	2^-	2^-	21	3.7	5.1	3.4
	500.216(4)[c]		500.3(3)	500.4(5)		3^-[c]	$(3^-, 4^+)$	8	0.9	1.8, 5.4	–, –
501.809(3)	501.812(3)	501.9(3)			2^-	2^-					
518.577(3)	518.578(3)					2^+					
519.517?(3)	519.519(3)	522.5(4)	519.1(4)	519.5(4)	(3^+)	$(3)^+$	(4^+)	3	0.5	3.4	–
524.217?(2)	524.202(8)				(3^+)	$(3)^+$					
			534.9(9)					4			
542.593?(7)	542.591(2)				(2^+)	$(2)^+$					
546.1(4)	*544.675(3)*[c,d]	545.37(16)	544.6(3)	544.4(3)	(2^-)	2^-[c,d]	2^-	35	8.0	5.9	9.4
557.8(5)		557.8(5)	555.7(4)					4			
	561.855(5)[c]			561.8(9)		5^+[c]	(5^+)		0.5	0.9	7.0

TABLE I. *(Continued.)*

E_x(keV)					J^π			$(d\sigma/d\Omega)^{20^\circ}$ (μb/sr)		$G_{\mathrm{LJ}}^{(1)}(10^{-3})$	$G_{\mathrm{LJ}}^{(2)}(10^{-3})$
NDS [3]	(n,γ) [1][a]	(d,p) [11]	(d,p)	$(\vec{d},\alpha)$	NDS [3]	Ref. [1]	$(\vec{d},\alpha)$	(d,p)	$(\vec{d},\alpha)$	$(\vec{d},\alpha)$	$(\vec{d},\alpha)$
572.4(7)		572.4(7)	570.9(4)					2			
				574.6(7)			(2^-)		0.6	0.9	0.6
578.97(23)		578.97(23)	578.4(3)		(0 to 3)$^-$			19			
591.9(4)		591.9(4)	591.5(3)	590.7(4)			2^-	5	2.7	6.3	1.5
600.1(6)			598.4(8)					2			
		605.73(17)	604.4(3)	604.1(5)			$(3^+, 4^-)$	11	0.4	1.0, 0.6	0.8, 1.7
	620.521(6)[d,e]	619.9(4)	620.5(3)	620.5(3)		3^-[d,e]	$4^-, 5^+$	6	1.7	2.1, 6.3	0.3, 0.0
		639.55(21)	639.7(3)	639.6(3)			$5^+, (4^-)$	8	3.1	10.5, 3.2	8.8, 9.1
		656.42(22)	657.3(3)					14			
				662.3(4)			(4^-)		3.6	3.2	9.1
		667.5(4)	667.9(3)	669.2(4)			$4^-, (3^+)$	11	3.1	2.4, 3.1	14.3, 11.6
		677.49(23)	677.8(3)					19			
				686.9(14)			(1^-)		0.2	1.2	–
		694.5(5)	690.5(3)					3			
			698.0(3)					1			
	708.548(5)[d]	707.7(4)	708.1(3)	708.6(4)		2^-[d]	(2^-)	7	2.0	3.4	1.0
		719.1(4)	718.7(3)	718.0(4)			4^-	8	2.6	1.0	14.6
		746.3(3)	748.3(4)	749.2(3)			2^-	11	5.8	21.4	1.6
		759.0(3)	762.7(3)	761.0(5)			(4^-)	20	2.1	1.3	9.4
		772.6(4)	773.8(3)					8			
			784.3(3)					1			
		799.7(8)	801.6(5)					3			
		808.7(3)	813.4(3)					27			
		819.2(3)	823.3(3)					13			
		834.2(9)	835.1(5)					4			
		853.8(4)	858.8(3)					4			
		872.4(3)	876.8(3)					18			
		879.4(6)	883.2(3)					12			
		888.00(14)	891.9(4)					5			
		897.4(5)	901.3(3)					6			
		908.2(6)	908.4(3)					4			
		921.2(5)	924.1(6)					2			
		934.0(8)									
		948.11(18)	954.6(4)					61			
			962.2(6)					20			

[a]Not all states from (n,γ) are listed here. For a complete list, see Table VI. The energies written in italic are seen only in the new (n,γ) evaluation reported in this paper.
[b]Used to calibrate the new (d,p) measurement.
[c]From (n,γ) reported in this paper, see Table VI, and used to calibrate the new $(\vec{d},\alpha)$ measurement.
[d]From (n,γ) reported in this paper, see Table VI, and used to calibrate the new (d,p) measurement.
[e]Spin assignment 3^- from (n,γ) not supported by $(\vec{d},\alpha)$.

2. ^{196}Pt$(\vec{d},\alpha)^{194}$Ir *measurement*

We measured the reaction ^{196}Pt$(\vec{d},\alpha)^{194}$Ir at nine angles between 10° and 50°. At all angles, separate spectra for deuteron spin up and spin down were recorded with periodic spin-flip. The target consisted of 40 μg/cm^2 metallic platinum (97% ^{196}Pt), evaporated on an 8 μg/cm^2 carbon backing. Figure 2 shows the spin up and spin down spectra for ^{196}Pt$(\vec{d},\alpha)^{194}$Ir at $E_d = 18$ MeV and a laboratory angle of 25°, both with nearly identical recording time. The effect of the polarization is clearly visible. The FWHM is 8 keV. In Fig. 1, the energy calibrated spectrum of 25° is shown (sum of spin up and spin down spectra). Figure 3 shows typical angular distributions of the cross section $d\sigma(\theta)/d\Omega$ and the analyzing power $A_y(\theta)$ for this reaction (see Sec. II A4). Note the low cross sections in the 1 μb/sr region. Because of the low cross section of this reaction and the appreciable energy loss of the outgoing α particles in the target material, which required the use of a very thin target, this was a challenging experiment with about 6 h measuring time for each of the 18 spectra.

3. *Formalism of the two-nucleon pickup reaction*

In $(\vec{d},\alpha)$ reactions, the spin of the transferred nucleon pair is $S = 1$ with the magnetic substates $m_s = +1, 0, -1$. Since we have zero spin for the even-even target nucleus ^{196}Pt,

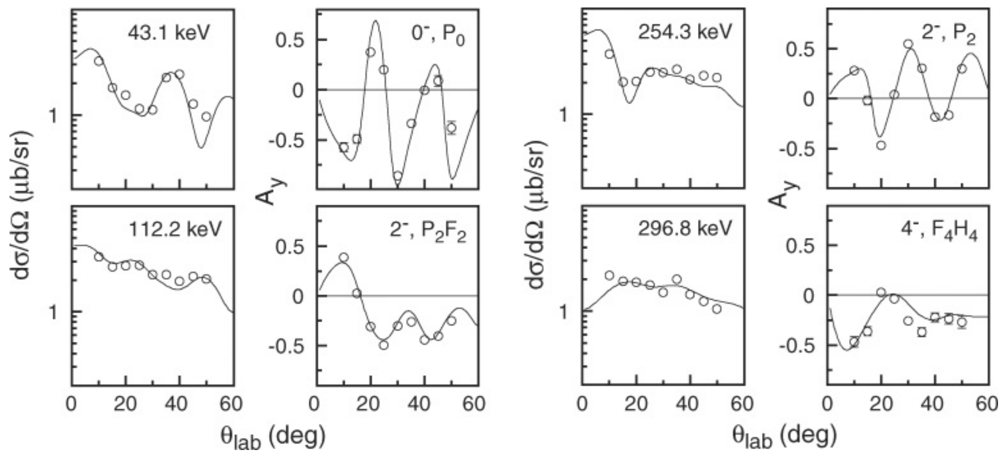

FIG. 3. Characteristic angular distributions of four states observed in the ^{196}Pt($\vec{d},\alpha$)^{194}Ir reaction. The measured absolute cross sections $d\sigma(\theta)/d\Omega$ and the analyzing powers $A_y(\theta)$ are plotted with the results of DWBA calculations (solid lines). The excitation energy, J^π, and L_J are given for each state. All angular distributions of ($\vec{d},\alpha$) are shown in Fig. 6.

the transferred angular momentum is identical to the angular momentum J of the respective excited state in ^{194}Ir. The values of J are restricted by the relation $\vec{J}=\vec{L}+\vec{S}$ between the transferred total, orbital, and spin angular momenta $\vec{J}$, $\vec{L}$, and $\vec{S}$. Thus we have to consider $J=L-1, L$, and $L+1$ transfers. The number of transfers L contributing to an actual state is further restricted by parity conservation: because of the positive parity of the target nucleus, the parity of the respective excited state in ^{194}Ir is determined by the transferred orbital angular momentum $L: \pi=(-1)^L$.

Consequently, states of natural parity $\pi=(-1)^J$ are populated by one transfer only, $L=J(\Delta S=0)$. For states of unnatural parity $\pi=-(-1)^J$, there are two different allowed L transfers, $L=J-1$ and $L=J+1$, both of which may contribute. Their (polarization dependent) cross sections add incoherently. Thus, in each case, we have L-characteristic angular distributions of the differential cross section and LJ-dependent angular distributions of the vector analyzing power. For the negative parity states, for example, we have to consider $L=1$ transfer to $J^\pi=0^-, 1^-$, and 2^- states; $L=3$ transfer to $J^\pi=2^-, 3^-$, and 4^- states; and $L=5$ transfer to $J^\pi=4^-, 5^-$, and 6^- states.

A summary of the relations between L transfers and J^π is given in Table II. An L transfer leading to a final state with total momentum J will be characterized in the following via L_J. For example, an $L=3$ transfer to a $J^\pi=2^-$ state is an F_2 transfer.

4. Data evaluation

In contrast to one-nucleon transfer reactions (with transferred spin $S=1/2$), two-nucleon transfer reactions with transferred spin $S=1$, as in ($\vec{d},\alpha$), have considerable tensor analyzing powers. The measured cross sections $\sigma_+(\theta)$ and $\sigma_-(\theta)$ (for spin up and spin down) include contributions due to the tensor polarization of the beam of $P_{yy}=65(5)\%$. In the experimental data analysis, we do not care about the tensor polarization and calculate experimental differential cross sections and vector analyzing powers as for a purely vector polarized beam:

$$\begin{aligned} d\sigma(\theta)/d\Omega &= [\sigma_+(\theta)+\sigma_-(\theta)]/2, \\ A_y(\theta) &= [\sigma_+(\theta)-\sigma_-(\theta)]/(3P_y)\cdot\frac{1}{d\sigma(\theta)/d\Omega}. \end{aligned} \tag{1}$$

These are the quantities which are shown as experimental data in the figures of the angular distributions. The correction for the tensor polarization is introduced on the level of the distorted-wave Born analysis (DWBA) with the code CHUCK3 [12], calculating the theoretical $d\sigma(\theta)/d\Omega^*$ and $A_y(\theta)^*$ curves from theoretical differential cross sections $\sigma^{\mathrm{LJ}}(\theta)$, vector analyzing powers $A_y^{\mathrm{LJ}}(\theta)$, and tensor analyzing powers $A_{yy}^{\mathrm{LJ}}(\theta)$ for the respective LJ transfers:

$$\begin{aligned} d\sigma(\theta)/d\Omega^* &= \sum_L G_{\mathrm{LJ}}\sigma^{\mathrm{LJ}}\cdot\left[1+\frac{1}{2}P_{yy}A_{yy}^{\mathrm{LJ}}\right], \\ A_y(\theta)^* &= \sum_L G_{\mathrm{LJ}}\sigma^{\mathrm{LJ}}A_y^{\mathrm{LJ}} \\ &\quad\times\left[1+\frac{1}{2}P_{yy}A_{yy}^{\mathrm{LJ}}\right]\cdot\frac{1}{d\sigma(\theta)/d\Omega^*}, \end{aligned} \tag{2}$$

TABLE II. Relation between J^π of the states in ^{194}Ir and the allowed L transfers in the ^{196}Pt($\vec{d},\alpha$)^{194}Ir reaction. States of natural parity $\pi=(-1)^J$ are populated by $L=J$ transfer only; states of unnatural parity $\pi=-(-1)^J$ may be populated by two different L transfers, $L=J-1$ and $L=J+1$.

L			J^π			
S/0	0^+	1^+				
P/1	0^-	1^-	2^-			
D/2		1^+	2^+	3^+		
F/3			2^-	3^-	4^-	
G/4				3^+	4^+	5^+
H/5					4^-	5^-
I/6						5^+

TABLE III. Optical potential parameters used in the DWBA calculations, with the finite range parameter FNRG = 0.4.

	d	α
V_r (MeV)	104.90	170.80
$4W_D$ (MeV)	53.85	
W_0 (MeV)		24.45
V_{so} (MeV)	6.61	
r_r (fm)	1.11	1.16
r_D (fm)	1.25	
r_0 (fm)		0.98
r_{so} (fm)	1.07	
R_c (fm)	1.15	1.40
a_r (fm)	0.97	0.89
a_D (fm)	1.20	
a_0 (fm)		0.97
a_{so} (fm)	0.66	
nlc	0.54	0.20

where $G_{\rm LJ}$ is the spectroscopic strength of the specific transfer. As shown above, in the case of the population of ^{194}Ir states with unnatural parity, two different L transfers may contribute. The angular distributions of the data are compared with these calculations, using the fitting routine MINUIT [13] to determine spectroscopic factors.

The optical potential parameters used for the DWBA calculations with CHUCK3 are listed in Table III.

Starting with potentials known from the compilation of Daehnick *et al.* [14], we fitted the parameters to reproduce states with one L_J transfer only.

The two-nucleon transfer was calculated according to Refs. [15–17] as a one-step cluster transfer of a deuteron, neglecting sequential transfer processes, which are supposed to be weak. We used the same potentials for the transferred deuteron as for the incoming deuteron projectile.

A total of 38 levels have been observed up to 761 keV. Above this energy, the level density is too high for a reliable analysis. For 16 levels, an unambiguous J^π assignment was obtained; and for nearly all levels, J^π values are proposed. The assignment was done by fitting all possible L_J transfers up to $J = 6$ and inspection of the χ^2 values. All angular distributions are given in Fig. 6 in the Appendix. The results of the $(\vec{d}, \alpha)$ measurement are summarized in Table I. The excitation energies are the average values of all spectra. The energy calibration was done using well-known level energies from NDS [3], Ref. [1], and the (d, p) reaction. $G^{(1)}_{\rm LJ}$ and $G^{(2)}_{\rm LJ}$ refer to the spectroscopic strength of both possible transfers in the case of unnatural parity, ordered by the L value. For example, at a 2^- state with possible P_2 and F_2 transfer, $G^{(1)}_{\rm LJ}$ stands for the $P_2(\Delta L = 1, \Delta S = +1)$ strength and $G^{(2)}_{\rm LJ}$ stands for the $F_2(\Delta L = 3, \Delta S = -1)$ strength.

B. Evaluation of the thermal neutron capture measurements above 500 keV

In an earlier paper, partial experimental results were reported based on the low-energy γ-ray and conversion electron measurements from thermal neutron capture at the ILL Grenoble research reactor, namely, the reactions ^{193}Ir$(n, \gamma)^{194}$Ir and ^{193}Ir$(n, e^-)^{194}$Ir [1], measured with the GAMS and BILL spectrometers, respectively. Table II of that earlier paper contains the results of transition energies from 22 to 500 keV.

The ILL Grenoble report on thermal neutron capture in ^{193}Ir [18] includes the γ-ray spectrum from 37 to 1530 keV. Thermal neutron capture cross sections for several iridium isotopes are large enough to observe multiple successive neutron capture. The cross sections of ^{193}Ir and ^{194}Ir are 111 and 1500 b, respectively. Taking also into account a value of $T(1/2) = 19.15$ h for ^{194}Ir and 2.5 h for ^{195}Ir, an isotopic assignment of observed γ lines was made. Based on these data, a paper on the structure of ^{195}Ir was published [19]. In principle, transitions observed in the thermal neutron capture on the ^{193}Ir target and not assigned to ^{195}Ir can be considered as being ^{194}Ir transitions. Sections 2.2 and 2.3 of the earlier ^{194}Ir paper [1] contain more details concerning the γ-ray and internal conversion electron measurements at the ILL Grenoble research reactor.

To proceed with the further development of the ^{194}Ir level scheme, the γ and conversion electron data in the energy region 500–680 keV were additionally evaluated. γ data are based on Ref. [18], and conversion electron data are taken from the same measurements presented up to 500 keV in Ref. [1]; however, this interval of the conversion electron spectrum was not published earlier. Multipolarities were determined for many of the transitions up to 689 keV. The results are presented in Table IV of the present work and listed in seven columns similar to those used for the 22–500 keV interval in Ref. [1]. The γ transition data for the 689–800 keV interval are presented in Table V taken from the ILL Grenoble report [18]. This report contains also a number of transitions with higher energies from 800 to 1530 keV.

However, we keep in mind the following limitations: (a) it seems to be reasonable to develop the ^{194}Ir level scheme only up to about 800–1000 keV, since the confidence of higher levels decreases rather quickly with increasing level energy, and (b) the paper on the ^{195}Ir level structure is based on the same experimental measurements as used now for the ^{194}Ir study. We believe that the criteria for isotopic assignment of transitions are only partially reliable in our case. For the region above 800 keV, it is problematic to say which transitions could be uniquely attributed either to ^{194}Ir or ^{195}Ir.

III. LEVEL SCHEME

A. General considerations

Highly complex nuclear level schemes in the transitional deformation region and especially for odd-odd nuclei present special problems even below 1000 keV. Comments on previous investigations of ^{194}Ir and other transitional nuclei such as ^{192}Ir, ^{196}Au, and ^{152}Eu may be of interest [1,20–22]. In this subsection, we emphasize the general approaches to the present development of the ^{194}Ir level scheme. The arguments for it are associated with the existing sets of data. In the earlier ^{194}Ir publication [1], 38 levels with spin values from 0 to 4 were presented below 543 keV. From these, we consider

TABLE IV. γ-ray and conversion electron data from 500 to 689 keV (extension of Table 2 from Ref. [1]; first two columns slightly reevaluated version of Ref. [18]).

$E_\gamma(\Delta E_\gamma)$ GAMS (keV)	$I_\gamma(\Delta I_\gamma)$ (rel.)	$E_e(\Delta E_e)$ BILL (keV)	$I_e(\Delta I_e)$ (rel.)	$\alpha(\Delta\alpha)_{\text{exp.}}$	Multi-polarity	Assignment $E_\text{i} - E_\text{f}$ (keV)
500.66(3)	33.7(91)	500.694(22)	1.62(23)	0.048(15)	$M1 + E2$	639.4–138.7
501.041(16)	49.9(53)	501.053(17)	2.59(21)	0.052(7)	$M1 + E2$	
503.33(11)	15.7(44)	503.172(19)	0.80(8)[a]	0.05(2)	$M1$, $E2$	
505.16(5)	22.9(33)	–				
505.69(3)	24.5(49)	505.72(3)	1.72(34)	0.07(2)	$M1$	
506.54(5)	25.6(36)	506.549(25)	1.54(23)	0.060(12)	$M1$	
509.934(27)	77.7(92)	509.981(17)	3.57(30)	0.046(6)	$M1 + E2$	
513.017(14)	68.4(53)	513.050(19)	3.15(32)	0.046(6)	$M1 + E2$	708.5–195.5
518.056(12)	57.0(30)	518.100(16)	3.08(22)	0.054(5)	$M1$	
520.35(7)	20.1(58)	520.161(29)	1.03(20)	0.051(18)	$M1 + E2$	669.4–148.9
520.57(6)	72.0(51)	–	⩽0.6	⩽0.008	$E1$	669.4–148.9
520.892(21)	73.0(61)	520.879(20)	2.12(23)[a]	0.029(4)	$M1 + E2$	
521.191(7)	72.7(75)	521.18(3)	1.02(22)	0.014(4)	$E2$	670.1–148.9
522.61(5)	17.2(26)	522.458(25)	0.96(20)[a]	0.056(14)	$M1$	
525.55(4)	23.3(29)	–				
525.98(3)	16.8(30)	–				
527.18(5)	19.5(28)	527.182(22)	1.15(21)[a]	0.059(13)	$M1$	639.4–112.2 722.8–195.5
528.34(6)	16.4(27)	528.35(8)	0.50(26)	0.030(16)	$M1$, $E2$	
530.26(6)	26.1(43)	–				
530.77(5)	60.9(26)	530.75(4)	3.35(23)	0.055(5)	$M1$	
531.388(17)	44.1(21)	531.38(4)	2.29(18)	0.052(5)	$M1$	670.1–138.7
533.27(5)	15.0(27)	–				
534.10(5)	20.4(25)	–				
534.893(29)	20.3(36)	534.84(4)	0.47(7)[a]	0.023(5)	$E2$, $E2 + M1$	
535.94(3)	23.8(78)	–				
536.339(13)	61.9(42)	536.35(4)	3.16(25)	0.051(6)	$M1$	
538.030(27)	21.5(58)	–				722.8–184.7
541.60(6)	9.8(24)	541.63(5)	0.85(30)	0.087(37)	$M1$	
542.12(7)	11.5(26)	542.10(5)	1.00(25)	0.087(29)	$M1$	
544.34(11)	14.0(29)	544.47(4)	1.34(23)	0.096(25)	$M1$	
546.23(5)	28.4(48)	546.35(5)	1.11(30)	0.039(12)	$M1$, $M1 + E2$	
546.902(15)	95.6(53)	546.95(4)	4.88(34)	0.051(4)	$M1$	
547.558(12)	123.5(49)	547.57(3)	5.93(36)	0.048(3)	$M1$	708.5–161.0
548.67(10)	11.4(49)	548.63(4)	1.14(24)	0.10(5)	$M1$	
548.998(22)	44.3(26)	549.12(6)	1.06(42)	0.024(10)	$E2$	
551.04(4)	23.7(43)	551.11(4)	1.54(18)	0.065(14)	$M1$	
552.080(17)	64.3(58)	552.09(3)	3.34(30)	0.052(7)	$M1$	
553.77(5)	19.3(39)	–				738.3–184.7
554.392(24)	39.0(83)	554.43(4)	1.37(18)	0.035(9)	$M1$, $M1 + E2$	
556.76(7)	34.4(45)	556.71(4)	1.24(26)	0.036(9)	$M1$, $M1 + E2$	
557.10(3)	64.7(58)	557.04(4)	2.46(42)	0.038(7)	$M1 + E2$	639.4–82.3 669.4–112.2
557.73(3)	45.5(65)	557.84(4)	1.27(18)	0.028(6)	$M1 + E2$	
558.07(19)	19.9(48)	–				670.1–112.2
558.54(3)	47.4(85)	558.49(3)	2.65(45)	0.056(14)	$M1$	
–	⩽10	560.99(3)	3.10(31)	⩾0.31	$E0$, $M2$	
565.02(4)	17.6(23)	565.034(18)	1.27(23)	0.072(16)	$M1$	708.5–143.6
566.360(26)	29.9(46)	566.39(4)	1.64(23)	0.055(11)	$M1$	
567.42(4)	19.4(23)	567.43(4)	1.77(32)	0.091(19)	$M1$	
568.444(16)	55.2(44)	568.43(3)	2.65(19)[a]	0.048(5)	$M1$	
569.779(13)	63.6(28)	569.76(4)	3.12(54)	0.049(9)	$M1$	
570.69(4)	28.5(30)	570.69(3)	1.85(22)[a]	0.065(10)	$M1$	
574.84(4)	41.4(45)	574.80(4)	2.07(30)[a]	0.050(9)	$M1$	

TABLE IV. *(Continued.)*

$E_\gamma(\Delta E_\gamma)$ GAMS (keV)	$I_\gamma(\Delta I_\gamma)$ (rel.)	$E_e(\Delta E_e)$ BILL (keV)	$I_e(\Delta I_e)$ (rel.)	$\alpha(\Delta\alpha)_{\text{exp.}}$	Multi-polarity	Assignment $E_\mathrm{i}-E_\mathrm{f}$ (keV)
575.691(10)	118.0(65)	575.70(3)	6.14(18)	0.052(3)	$M1$	722.8–147.1
576.819(18)	45.9(64)	576.77(3)	3.81(27)	0.083(13)		738.3–161.5
578.959(25)	36.7(51)	578.85(9)	1.28(26)	0.035(8)	$M1$, $M1+E2$	
579.62(4)	25.1(26)	579.66(6)	1.58(32)	0.063(14)	$M1$	
580.909(21)	41.9(23)	581.05(4)	1.38(20)[b]	0.033(5)	$M1+E2$	
582.71(13)	20.9(34)	582.80(5)	0.92(27)	0.044(15)	$M1$, $M1+E2$	
584.81(3)	27.6(30)	584.73(4)	1.21(20)	0.044(9)	$M1$	
588.40(5)	36.7(73)	–				
593.13(6)	17.9(28)					
		593.56(5)	1.12(20)			
593.66(9)	13.9(34)					
596.28(8)	20.7(26)	596.00(7)	0.46(17)	0.022(9)	$M1+E2$	639.4–43.1 708.5–112.2
597.13(4)	31.7(32)	597.05(6)	0.82(18)	0.026(6)	$M1+E2$, $E2$	
598.08(16)	49.1(72)	597.69(6)[b]	0.69(17)	0.014(4)	$E2$	
599.65(3)	64.3(57)	599.77(6)	2.12(40)	0.033(7)	$M1$	
600.470(8)	185.6(64)	600.47(5)	7.05(50)	0.038(3)	$M1$	
601.871(23)	37.8(46)	601.90(6)	1.32(22)	0.035(7)	$M1$	
603.04(10)	111.4(67)	602.99(6)	0.86(17)	0.0077(16)	$E1$	
603.95(5)	20.7(27)	–	⩽0.45	⩽0.022	$E2$, $E1$	
605.39(4)	29.1(46)	605.29(6)	1.19(18)	0.041(9)	$M1$	
605.76(9)	22.5(22)	605.66(6)	1.06(17)	0.047(9)	$M1$	605.5–0.0
606.880(23)	54.3(32)	606.90(6)	1.85(19)	0.034(4)	$M1$	
607.57(16)	24.3(77)	607.329(6)	1.09(17)	0.045(16)	$M1$	
608.688(27)	47.8(27)	608.64(6)	1.77(20)	0.037(5)	$M1$	
609.76(9)	134.2(71)	609.67(6)	0.47(12)[a]	0.0035(9)	$E1$	
610.15(4)	36.2(50)	610.22(6)	1.38(20)[a]	0.038(8)	$M1$	
610.762(8)	145.9(75)	610.76(6)	5.40(27)	0.037(3)	$M1$	
611.27(9)	22.4(53)	611.26(6)	1.39(17)	0.062(16)	$M1$	
612.76(7)	97.0(59)	–	⩽0.5	⩽0.005	$E1$	
613.48(8)	28.6(49)	613.66(10)	0.74(17)	0.026(7)	$M1+E2$	
614.58(8)	28.6(56)	614.55(7)	0.77(22)	0.027(9)	$M1+E2$	
615.25(13)	37.4(79)	615.36(7)	0.94(20)	0.025(7)	$M1+E2$	
615.73(11)	59.7(51)	615.76(8)	1.13(33)	0.019(6)	$E2$	
616.40(9)	45.5(44)	616.30(7)	0.68(22)	0.015(5)	$E2$	
617.102(29)	58.5(63)	617.12(7)	1.64(16)	0.028(4)	$M1+E2$	
618.07(18)	21.6(37)	–				
618.46(7)	17.2(30)	–				
619.28(7)	21.1(49)	–				
622.67(5)	44.0(112)	622.67(8)	1.50(24)	0.034(10)	$M1$, $M1+E2$	
623.25(3)	48.5(117)	623.23(7)	1.65(30)	0.034(10)	$M1$, $M1+E2$	
623.80(7)	50.8(71)	623.77(8)	2.13(40)	0.042(10)	$M1$	
624.72(12)	62.3(77)	625.01(8)[b]	0.87(28)	0.014(5)	$E2$	
626.211(21)	49.1(48)	626.21(9)	1.82(22)	0.037(6)	$M1$	669.4–43.1 708.5–82.3
629.06(12)	18.0(30)	629.10(8)	1.08(20)	0.060(15)	$M1$	
630.37(8)	18.9(25)	630.52(9)	0.60(18)	0.032(9)	$M1$	
631.48(7)	19.2(29)	631.16(8)[b]	0.75(17)[a]	0.039(11)	$M1$	
635.33(10)	75.9(45)	–	⩽0.5	⩽0.006	$E1$	
635.90(11)	20.5(43)	–				
637.12(8)	41.7(93)	637.19(11)	0.46(20)	0.011(5)	$E2$	
639.91(4)	61.4(62)	640.04(9)	1.90(20)	0.031(5)	$M1$	
642.046(21)	75.1(59)	642.05(9)	2.40(30)	0.032(4)	$M1$	
643.800(27)	47.9(55)	643.79(9)	1.96(22)	0.041(7)	$M1$	
646.96(6)	25.2(32)	646.96(10)	0.86(26)	0.034(11)	$M1$	

TABLE IV. *(Continued.)*

$E_\gamma(\Delta E_\gamma)$ GAMS (keV)	$I_\gamma(\Delta I_\gamma)$ (rel.)	$E_e(\Delta E_e)$ BILL (keV)	$I_e(\Delta I_e)$ (rel.)	$\alpha(\Delta\alpha)_{\text{exp.}}$	Multi-polarity	Assignment $E_\text{i} - E_\text{f}$ (keV)
648.647(27)	63.8(57)	648.59(9)	2.11(20)	0.033(4)	$M1$	
649.21(7)	32.4(45)	649.03(10)	0.62(17)	0.019(6)	$M1 + E2$	
651.172(16)	62.2(89)	651.23(10)	1.80(18)	0.029(5)	$M1$	
652.99(7)	25.9(34)	653.16(10)	0.96(20)	0.037(9)	$M1$	
653.93(10)	16.6(36)	–				738.3–84.3
656.82(7)	40.4(52)	656.69(11)	1.41(28)	0.035(8)	$M1$	
659.136(27)	45.7(60)	659.09(11)	1.37(26)	0.030(7)	$M1$	
662.51(11)	19.6(35)	662.30(11)	1.16(27)	0.059(17)	$M1$	
663.27(8)	19.7(32)	663.11(11)	0.71(10)[a]	0.036(8)	$M1$	
665.91(4)	47.3(31)	666.01(11)	1.09(23)	0.023(5)	$M1 + E2$	
675.08(6)	22.6(140)	675.12(13)	0.57(17)	0.025(17)	$M1$	
676.66(14)	16.3(41)	–				
677.02(12)	24.2(60)	677.00(13)	0.82(19)	0.034(11)	$M1$	
677.42(16)	16.0(45)	–				
677.99(7)	51.7(39)	678.01(12)	1.40(17)	0.027(4)	$M1$	
679.20(20)	9.0(64)	–				
679.90(8)	31.0(33)	680.07(13)	0.56(18)	0.018(6)	$M1 + E2$	
680.84(5)	46.3(37)	680.73(13)	0.65(16)	0.014(4)	$E2, M1 + E2$	
684.76(27)	53.6(149)	–	$\leqslant$0.5	$\leqslant$0.009	$E1$	
685.79(7)	33.2(71)	685.79(16)	0.96(16)	0.029(8)	$M1$	
687.10(4)	34.4(104)	687.05(13)	0.96(20)	0.028(10)	$M1$	
688.97(6)	48.6(35)	688.93(14)	1.02(27)	0.021(6)	$M1$	

[a]The intensities of superimposed conversion lines from other transitions are subtracted.
[b]Questionable conversion electron lines.

35 levels to have enough confidence to be included in the new level scheme. New levels are established mainly below 750 keV with spin values from 0 to 5 given with their depopulation in Table VI. In the energy interval below 550 keV, $(\vec{d}, \alpha)$ results (Table I) allow us to establish new levels with spins higher than 3 such as the 5^+ level at 161.5 keV.

In most cases, spins-parities in Table VI are well supported by those from the $(\vec{d}, \alpha)$ data. The new (d, p) data (Sec. II A1), evidently of better sensitivity and energy resolution than those published earlier, help to find, e.g., the new 486.1 keV 2^- level. A few new low-lying positive parity levels (263.8, 293.2, 361.4 keV) are established via a careful analysis of transition and multipolarity data; it is understandable that they cannot be intense enough in direct level observations due to neutron or deuteron reactions. Three levels, at 371.3, 413.0, and 524.2 keV, are removed from the level scheme of Ref. [1] because their confidence is too weak.

Let us emphasize an evident asymmetry of the two parities at low energies: there are 10 and 34 levels of positive and negative parity, respectively, between 0 and 543 keV.

The new (d, p) reaction data show good quality both at lower and higher energies and better energy calibration up to about 962 keV. The $(\vec{d}, \alpha)$ reaction data end at about 761 keV. They help to establish new levels and to assign spin-parity values.

The primary γ-ray spectrum from thermal neutron capture is available up to about 1423 keV excitation energy (see Table 1 in Ref. [11]). If one counts mainly low-energy excitations, probably more than 90% of the 1^- and 2^- levels are detected with this method (at low energies, an evident exception is the 195.5 keV level). If level doublets do not disturb the picture (e.g., 245.1 keV 3^- and 245.5 keV 0^-, 578.5 keV 3^- and 579.1 keV 2^-), presumably a few 0^- and 3^- levels can be established with the aid of primary γ rays.

The average resonance capture (ARC) spectra have been measured for excitation energies 0–600 keV [1]. In the present paper, the levels and their spins at 544 and 578–579 keV are supported by these data. Most conclusions from these data for lower energies (e.g., evident existence of a close doublet 337.5 keV 1^- and 337.6 keV 2^-) are confirmed. Even though intensity errors are sometimes larger than reported in the published table of the ARC data, most conclusions concerning the existence of $(0\text{–}3)^-$ levels at low energies can be assumed to be correct. For positive parity levels, the ARC results have too small sensitivity.

For the existence of "old" and "new" levels, these general considerations are assumed to give a satisfactory explanation in most cases. For a few special features, limited argumentation on a few specific levels is given in Sec. III B.

The computer program LEVFIT [23] was used to place the transitions into the level scheme and to calculate the level energies with a least squares fit. For very high level densities, automatic placement of transitions sometimes leads to mistakes; therefore the results are checked with the following criteria:

(i) Usually, only $E1$, $M1$, and $E2$ multipolarities are accepted. $M2$ or higher multipolarities can be involved in

TABLE V. γ-ray energies and intensities for energies 689–800 keV (from Ref. [18]).

E_γ (keV)	I (rel.)	$E_i - E_f$ (keV)
689.63(16)	24.1(58)	
690.76(9)	35.9(80)	
691.11(9)	47.5(76)	
692.02(6)	71.5(87)	
698.623(15)	113.2(83)	
700.11(13)	27.0(116)	
700.59(14)	45.5(43)	
701.45(10)	30.8(47)	
704.47(12)	32.1(64)	
706.54(4)	90.8(51)	
708.547(17)	234.3(87)	708.5–0.0
709.47(4)	66.3(63)	
710.20(7)	35.8(79)	
713.23(13)	35.5(123)	
713.77(5)	61.1(61)	
716.15(11)	30.1(66)	
717.21(6)	76.9(97)	
719.33(8)	32.6(84)	
720.96(13)	20.7(55)	
722.29(9)	61.7(52)	
722.93(10)	37.9(57)	
724.09(15)	19.4(48)	
725.39(8)	41.0(92)	
727.67(5)	37.6(147)	
731.97(13)	16.8(42)	
735.59(15)	23.9(54)	
738.25(10)	35.6(65)	
740.66(7)	49.6(58)	
743.87(4)	55.1(120)	
745.33(6)	57.8(87)	
747.465(26)	112.3(159)	
748.57(4)	64.7(297)	
749.933(29)	83.8(145)	
751.83(10)	42.7(64)	
753.14(9)	37.6(74)	
755.82(8)	33.2(57)	
757.49(4)	69.6(70)	
759.70(8)	34.4(73)	
761.33(3)	96.3(84)	
762.23(13)	45.5(52)	
763.37(9)	28.2(88)	
768.39(8)	32.0(49)	
769.82(12)	31.7(44)	
771.72(9)	41.4(50)	
773.92(10)	41.2(58)	
776.19(7)	36.3(47)	
781.49(10)	32.8(107)	
783.87(19)	29.4(60)	
785.511(28)	127.9(52)	
787.07(10)	64.3(111)	
787.72(6)	41.7(124)	
788.46(20)	56.2(81)	
788.98(5)	74.5(147)	
789.86(17)	38.6(63)	
795.08(12)	41.1(62)	
797.03(5)	84.6(114)	

special cases, e.g., in the decay of the 147.0 keV 4^+ level.

(ii) Possible doublets of transitions are treated individually.

(iii) Experimental multipolarities of strong and many medium intensity transitions are assumed to be highly secure.

They help to establish levels and to determine spin-parities. Multipolarities are checked individually for a number of transitions; e.g., clearly defined $E1$ transitions cannot be in place where $M1$ is expected.

Because of the high complexity of the spectra and the high level density, individual larger energy deviations of transitions are accepted. Some multipolarities of weaker transitions might be not correct if they are influenced by adjacent transitions. Consequently, some inconsistencies are allowed in Table VI.

The intensity values in columns 7, 9, and 10 are obtained using theoretical conversion coefficients and assuming minimal multipolarities of the transitions. For a limited number of strong transitions, experimentally determined $M1 + E2$ mixing ratios are used.

In the spin-parity determination, the general arguments are similar to those of Sec. 3 in the earlier work [1]. A few special points can be mentioned:

(i) The ground state is a 1^- level.

(ii) The short-lived isomeric level at 147.07 keV has spin-parity 4^+.

(iii) The ARC data provide reliable results for $1, 2, 3^-$ levels from 0 to 390 keV, and somewhat less reliable results between 390 and 590 keV, where a higher probability of doublets and larger intensity errors can influence our conclusions.

(iv) The $(\vec{d}, \alpha)$ data, in most cases, give spin-parities or limits for spin-parities, e.g., $2^-, 3^+$ for the 270.9 keV level.

(v) The multipolarity data for all located transitions are carefully analyzed, and a few interesting points are reported in Sec. III B.

Spin-parity assignments for almost all 38 levels observed in the $(\vec{d}, \alpha)$ data (Table I), up to about 600 keV, indicate good agreement with assignments of Table VI based mainly on level depopulation data and transition multipolarities. A few of presumably unambiguous assignments deserve special comment, as well as a few probable assignments. Well-established levels at 148.9, 270.9, and 394.8 keV are of interest; a level at about 591 keV deserves a comment despite its tentative character. See the next subsection.

For negative parity levels, one can optimistically state the completeness of the level scheme until 400 keV for $(0\text{–}4)^-$ levels. We are more sceptical for positive parity levels, since the $(\vec{d}, \alpha)$ data are not complete. One or two unknown 4^+ levels are possible, and unknown higher spin positive parity levels can exist.

B. Specific levels

We comment on the most important changes with respect to the earlier work at lower energies and a few characteristic

TABLE VI. Level scheme information for ^{194}Ir from low-energy ($\leqslant$800 keV) γ rays.

Level energy (keV)	Spin and parity	Pop. level (keV)	J^{π} pop. level	Trans. energy (keV)	γ int. (rel.)	Total int. (rel.)	Multi-pola-rity	Dep. int. (rel.)	Pop. int. (rel.)
0.0	1^-								9405
43.119(1)	0^-	0	1^-	43.119	133.1	1880.4	$M1(+E2)$	1880[a]	2485
82.336(1)	1^-	0	1^-	82.339	85.7	1040.0	$M1+E2$	1586	1201
		43	0^-	39.217	29.7	545.8	$M1(+E2)$		
84.285(1)	2^-	0	1^-	84.285	198.0	2229.0	$M1+E2$	2451	1884
		43	0^-	41.162	0.8	221.7	$E2$		
112.231(1)	2^-	0	1^-	112.230	345.1	1514.5	$M1+E2$	1943	1448
		82	1^-	29.890	6.9	276.7	$M1+E2$		
		84	2^-	27.927	1.0	151.7	$M1+E2$		
138.688(1)	1^-	0	1^-	138.686	138.2	370.8	$M1+E2$	1868	999
		43	0^-	95.575	137.4	1131.3	$M1(+E2)$		
		82	1^-	56.355	8.4	58.3	$M1+E2$		
		84	2^-	54.404	21.1	160.8	$M1+E2$		
		112	2^-	26.434	2.6	146.8	$M1$		
143.594(1)	0^-	0	1^-	143.594	109.7	357.0	$M1$	396	229
		82	1^-	61.225	6.8	38.6	$M1$		
147.074(1)	4^+	84	2^-	62.793	5.6	760.3	M2	1293[a]	1623
		112	2^-	34.829	0.3	532.2	M2		
148.935(1)	3^-	0	1^-	148.934	244.2	487.7	$E2$	636	303
		84	2^-	64.647	29.7	148.5	$M1$		
160.998(1)	1^-	0	1^-	160.996	71.6	175.8	$M1+E2$	1084[a]	1494
		43	0^-	117.880	73.6	364.7	$M1(+E2)$		
		82	1^-	78.666	9.7	133.3	$M1$		
		112	2^-	48.707	3.6	36.7	$M1+E2$		
		139	1^-	22.264	4.0	374.1	$M1$		
161.518(2)[b]	5^+								127
184.688(2)	3^-	0	1^-	184.687	156.9	229.2	$E2$	432	300
		84	2^-	100.407	22.0	160.4	$M1+E2$		
		149	3^-	35.723	1.8	42.7	$M1+E2$		
195.524(1)	2^-	0	1^-	195.519	35.6	49.2	$E2$	428[a]	518
		43	0^-	152.405	62.7	120.1	$E2$		
		82	1^-	113.192	8.4	45.5	$M1+E2$		
		84	2^-	111.246	5.7	32.2	$M1+E2$		
		112	2^-	83.291	6.8	79.8	$M1$		
		139	1^-	56.844	11.4	77.7	$M1+E2$		
		149	3^-	46.499	2.1	24.2	$M1$		
245.119(1)	3^-	0	1^-	245.115	24.0	28.3	$E2$	352	167
		82	1^-	162.774	40.9	70.3	$E2$		
		84	2^-	160.825	57.8	116.0	$M1+E2$		
		112	2^-	132.883	29.9	80.3	$M1+E2$		
		149	3^-	96.172	5.3	42.8	$M1+E2$		
		196	2^-	49.520	1.4	13.9	$M1$		
245.491(2)	0^-	0	1^-	245.491	51.9	78.0	$M1(+E2)$	78	71
254.161(1)	2^-	82	1^-	171.835	8.2	19.4	$M1$	1037	629
		84	2^-	169.874	25.9	62.2	$M1$		
		139	1^-	115.473	80.2	416.8	$M1+E2$		
		161	1^-	93.166	59.2	520.4	$M1$		
		185	3^-	69.460	4.2	17.8	$M1+E2$		
263.799(3)[c]	4^+	147	4^+	116.726[d]	17.4	88.2	$M1+E2$	116	50
		162	5^+	102.267[d]	4.0	27.6	$M1+E2$		
270.918(2)	3^+[e]	147	4^+	123.845	172.4	765.0	$M1+E2$	810	500
		162	5^+	109.400[d]	10.5	44.7	$E2$		
278.505(2)	2^-	0	1^-	278.502	302.1	409.4	$M1+E2$	514	134
		84	2^-	194.217	7.7	15.2	$M1+E2$		
		112	2^-	166.275	15.6	38.8	$M1$		

TABLE VI. *(Continued.)*

Level energy (keV)	Spin and parity	Pop. level (keV)	J^π pop. level	Trans. energy (keV)	γ int. (rel.)	Total int. (rel.)	Multi-pola-rity	Dep. int. (rel.)	Pop. int. (rel.)
		139	1^-	139.804	3.0	10.3	$M1$		
		149	3^-	129.571	4.0	16.3	$M1+E2$		
		161	1^-	117.503	4.8	24.2	$M1$		
293.242(3)[c]	4^+	147	4^+	146.169[d]	15.3	48.0	$M1$	48	31
296.633(2)	4^-	84	2^-	212.346	26.3	33.9	$E2$	67	60
		112	2^-	184.407	4.8	7.1	$E2$		
		185	3^-	111.938	4.7	26.1	$M1$		
		254	2^-	42.484[f]					
308.975(1)	1^-	0	1^-	308.975	97.1	123.2	$M1+E2$	424	120
		82	1^-	226.639	33.3	54.3	$M1+E2$		
		112	2^-	196.639	1.7	3.4			
		139	1^-	170.314	3.8	9.1	$M1+E2$		
		144	0^-	165.375	46.0	115.6	$M1$		
		161	1^-	147.979	7.8	23.8	$M1$		
		185	3^-	124.320	2.9	8.5	$E2$		
		196	2^-	113.447	15.0	86.1	$M1$		
314.075(2)	2^-	0	1^-	314.065	45.0	56.6	$M1+E2$	349	139
		82	1^-	231.751	6.5	10.3	$M1+E2$		
		161	1^-	153.054	84.6	243.7	$M1$		
		185	3^-	129.368	5.2	21.0	$M1$		
		245	3^-	69.009	4.0	17.2			
337.523(2)	1^-	0	1^-	337.531	104.4	126.6	$M1$	374	47
		43	0^-	294.411	12.7	16.6	$M1$		
		139	1^-	198.834	25.0	47.6	$M1+E2$		
		144	0^-	193.928	36.2	71.2	$M1(+E2)$		
		149	3^-	188.628	1.3	1.8			
		161	1^-	176.534	10.1	22.8	$M1$		
		196	2^-	141.953	6.1	20.3	$M1+E2$		
		245	0^-	92.019	7.4	67.2			
337.649(2)	2^-	43	0^-	294.531	69.4	76.4	$E2(+M1)$	407	54
		82	1^-	255.313	61.0	88.6	$M1+E2$		
		112	2^-	225.412	19.6	32.1	$M1+E2$		
		149	3^-	188.721	9.6	19.7	$M1+E2$		
		161	1^-	176.654	26.3	59.5	$M1$		
		185	3^-	152.960	8.1	23.4	$M1+E2$		
		254	2^-	83.419	8.6	100.4			
		279	2^-	59.142	1.2	7.4	$M1+E2$		
347.050(2)	3^-	0	1^-	347.064	15.2	16.2	$E2$	263	6
		82	1^-	264.744[d]	66.9[g]	76.3	$M1+E2$		
		112	2^-	234.817	75.6	118.6	$M1+E2$		
		149	3^-	198.101	9.6	18.3	$M1+E2$		
		185	3^-	162.366	8.6	22.2	$M1+E2$		
		196	2^-	151.526	4.0	11.7	$M1$		
361.382(4)[c]	4^+	147	4^+	214.327[d]	2.1	3.6	$M1$	105	37
		271	3^+	90.460[d]	10.7	101.8	$M1$		
377.009(3)	3^-	84	2^-	292.665	6.7	8.8	$M1+E2$	197	181
		112	2^-	264.744[d]	66.9[g]	94.3	$M1+E2$		
		149	3^-	228.070	20.5	33.1	$M1+E2$		
		161	1^-	215.991	5.5	7.0	$E2$		
		185	3^-	192.349	1.3	2.7			
		245	3^-	131.898	9.4	36.4	$M1$		
		254	2^-	122.847	3.3	15.0	$M1$		
390.963(2)	2^-[e]	0	1^-	390.961	98.3	112.4	$M1$	156	111
		139	1^-	252.288	18.6	27.3	$M1+E2$		
		254	2^-	136.803	4.5	16.1			

TABLE VI. *(Continued.)*

Level energy (keV)	Spin and parity	Pop. level (keV)	J^π pop. level	Trans. energy (keV)	γ int. (rel.)	Total int. (rel.)	Multi-pola-rity	Dep. int. (rel.)	Pop. int. (rel.)
394.880(3)[b]	4^-	84	2^-	310.590[d]	46.1	50.1	$E2(+M1)$	93	25
		112	2^-	282.646[d]	7.3	8.2	$(E1)$		
		149	3^-	245.943[d]	12.7	19.0	$M1+E2$		
		185	3^-	210.202[d]	4.9	8.7	$M1+E2$		
		245	3^-	149.777[d]	2.4	7.3			
407.019(3)	3^+	84	2^-	322.605	2.4	2.4		135	60
		147	4^+	259.949	10.7	15.3	$M1$		
		264	4^+	143.213[d]	3.9	12.8	$M1$		
		271	3^+	136.100	28.8	104.5	$M1$		
416.590(5)[b]	4^-	147	4^+	269.518[d]	7.7	7.9	$E1$	65	5
		185	3^-	231.901[d]	20.3	32.3	$M1$		
		297	4^-	119.958[d]	5.2	24.9	$M1+E2$		
419.611(3)	3^-	139	1^-	280.956	3.4	3.8		209	58
		196	2^-	224.085	30.6	50.4	$M1$		
		254	2^-	165.448	60.1	151.0	$M1$		
		361	4^+	58.037[d]	2.8	3.7			
423.727(2)	2^-	0	1^-	423.743	3.9	4.4	$M1$	291	15
		112	2^-	311.492	27.9	35.2	$M1+E2$		
		147	4^+	276.667	5.8	14.4			
		161	1^-	262.739	23.1	32.7	$M1+E2$		
		196	2^-	228.201	16.7	26.9	$M1+E2$		
		254	2^-	169.564	40.3	97.3	$M1$		
		279	2^-	145.221	18.6	59.3	$M1$		
		314	2^-	109.662	3.6	21.2	$M1+E2$		
436.296(2)	$1, 2^-$	0	1^-	436.281	10.4	11.6	$M1$	329	64
		82	1^-	353.963	87.3	103.6			
		112	2^-	323.858	5.5	6.8	$M1$		
		139	1^-	297.597	7.0	9.1	$M1+E2$		
		144	0^-	292.665	6.7	7.4	$M1+E2$		
		161	1^-	275.292	96.3	131.6	$M1+E2$		
		196	2^-	240.774	11.3	17.2	$M1+E2$		
		245	3^-	191.198	2.9	5.7			
		245	0^-	190.789	2.7	3.8	$M1+E2$		
		254	2^-	182.146	15.2	32.7	$M1$		
		395	4^-	41.416[d,f]	1.1				
467.209(3)	4–[e]	43	0–	424.207[f]	10.5	10.9	$E2$	252	2
		84	2^-	382.906	14.8	15.5			
		144	0^-	323.858[f]	5.5	5.9			
		161	1^-	306.240[f]	6.0	7.7	$M1$		
		162	5^+	305.687[d]	9.2	9.5			
		185	3^-	282.515	5.6	7.5	$M1+E2$		
		196	2^-	271.676	95.5	107.8	$E2$		
		279	2^-	188.628	1.3	1.8			
		297	4^-	170.588	3.6	8.7	$M1+E2$		
		309	1^-	158.249[f]	5.9	15.9	$M1$		
		338	2^-	129.571	4.0	10.9	$M1+E2$		
		361	4^+	105.814[d]	2.1	2.8			
		377	3^-	90.187	9.1	87.1			
486.067(3)[h]	2^-	84	2^-	401.782[d]	20.0	22.7	$M1+E2$	191	1
		112	2^-	373.845[d]	11.7	13.5	$M1+E2$		
		144	0^-	342.472[d]	16.7	17.8	$E2$		
		185	3^-	301.356[d]	5.4	7.0	$M1$		
		196	2^-	290.516[d]	8.6	11.4	$M1$		
		254	2^-	231.901[d]	20.3	32.3	$M1$		
		309	1^-	177.120[d]	6.1	13.7	$M1+E2$		

TABLE VI. *(Continued.)*

Level energy (keV)	Spin and parity	Pop. level (keV)	J^π pop. level	Trans. energy (keV)	γ int. (rel.)	Total int. (rel.)	Multi-pola-rity	Dep. int. (rel.)	Pop. int. (rel.)
		314	2^-	172.016[d]	3.9	9.3	$M1$		
		377	3^-	109.058[d]	4.6	27.6	$M1$		
		390	2^-	95.107[d]	4.3	35.7	$M1+E2$		
489.649(3)	2^-	82	1^-	407.325	21.8	24.7	$M1$	191	7
		84	2^-	405.351	18.9	21.4	$M1$		
		112	2^-	377.346	8.4	9.8			
		139	1^-	350.914	3.6	4.3			
		144	0^-	346.040	4.8	5.1			
		185	3^-	304.982	6.4	8.2	$M1$		
		254	2^-	235.493	13.6	21.3	$M1$		
		279	2^-	211.133	10.0	17.6	$M1+E2$		
		309	1^-	180.680	8.5	18.6	$M1$		
		314	2^-	175.608	3.5	8.1			
		338	1^-	152.118	3.3	9.7	$M1$		
		338	2^-	152.016	2.5	7.4	$M1$		
		391	2^-	98.698	4.6	34.9	$M1+E2$		
500.216(4)[h]	3^-	185	3^-	315.520[d]	4.2	5.3	$M1+E2$	86	15
		196	2^-	304.666[d]	23.2	29.7	$M1$		
		254	2^-	246.051[d]	6.7	10.1	$M1$		
		271	3^+	229.269[d]	8.9	9.4	$E1$		
		314	2^-	186.162[d]	15.2	31.7	$M1$		
501.812(3)	2^-	84	2^-	417.526	4.4	5.0	$M1$	228	2
		112	2^-	389.698	11.5	13.2	$M1+E2$		
		139	1^-	363.142	7.1	8.3	$M1$		
		144	0^-	358.200	4.8	5.0			
		161	1^-	340.813	130.0	156.8	$M1$		
		196	2^-	306.240	6.0	7.7	$M1$		
		254	2^-	247.655	7.9	11.8	$M1$		
		309	1^-	192.818	1.4	2.8	$M1$		
		377	3^-	124.777	3.9	17.1	$M1+E2$		
518.576(3)	2^+	82	1^-	436.281	10.4	10.5	$M1$	433	28
		147	4^+	371.502	359.4	378.3	$E2$		
		185	3^-	334.120	4.7	4.8	$E1$		
		196	2^-	323.037	4.1	4.2			
		271	3^+	247.655	7.9	11.8	$M1$		
		309	1^-	209.595	5.7	6.1	$E1$		
		338	1^-	181.069	7.5	8.1	$E1$		
		338	2^-	180.930	8.6	9.4	$E1$		
519.519(3)	$3, 4^+$	147	4^+	372.475	7.5	8.7	$M1$	140	26
		162	5^+	358.000	4.3	5.1			
		254	2^-	265.383	4.3	11.6			
		264	4^+	255.743	6.3	9.2	$M1$		
		271	3^+	248.599	40.8	60.6	$M1$		
		293	4^+	226.299	6.5	10.5	$M1$		
		407	3^+	112.500	6.3	34.6	$M1$		
519.788(2)[c]	$3, 4^-$	112	2^-	407.540[d]	12.7	13.3	$M1$	116	144
		149	3^-	370.866[d]	6.5	7.6	$M1$		
		185	3^-	335.095[d]	17.0	20.7	$M1+E2$		
		196	2^-	324.265[d]	31.0	33.4	$M1+E2$		
		254	2^-	265.625[d]	6.9	7.9	$(E1)$		
		297	4^-	223.211[d]	2.8	4.6	$M1$		
		314	2^-	205.743[d]	3.8	5.0	$(M1+E2)$		
		347	3^-	172.759[d]	2.5	5.9			
		361	4^+	158.411[d]	8.0	9.0	$E1$		
		377	3^-	142.778[d]	2.8	9.1	$M1$		

TABLE VI. *(Continued.)*

Level energy (keV)	Spin and parity	Pop. level (keV)	J^π pop. level	Trans. energy (keV)	γ int. (rel.)	Total int. (rel.)	Multi-pola-rity	Dep. int. (rel.)	Pop. int. (rel.)
542.591(2)	1, 2^+	82	1^-	460.250	133.3	134.5	$E1$	373	157
		84	2^-	458.294	69.8	70.5	$E1$		
		112	2^-	430.399	5.7	5.8			
		254	2^-	288.423	19.6	20.2	$E1$		
		271	3^+	271.676	95.5	131.8	$E2$		
		338	1^-	205.065	9.6	10.3	$E1$		
544.675(3)[h]	2^-	112	2^-	432.449[d]	7.4	8.2	$M1+E2$	179	9
		160	1^-	383.676[d]	60.7	69.8	$M1$		
		195	2^-	349.062[d]	3.5	4.2			
		245	3^-	299.567[d]	7.6	9.8	$M1+E2$		
		254	2^-	290.516[d]	8.6	11.4	$M1$		
		279	2^-	266.168[d]	5.0	7.0	$M1$		
		309	1^-	235.707[d]	15.1	23.7	$M1$		
		314	2^-	230.627[d]	4.4	7.1	$(M1)$		
		338	1^-	207.123[d]	5.2	9.4	$M1+E2$		
		391	2^-	153.750[d]	2.5	7.2	$(M1+E2)$		
		395	4^-	149.777[d]	2.4	4.8			
		407	3^+	137.645[d]	2.6	3.0			
		420	3^-	125.085[d]	3.0	12.9			
556.373(4)[c]	3^-	84	2^-	472.102[d]	36.0	39.1	$M1$	113	0
		112	2^-	444.250[d]	9.6	10.6			
		196	2^-	360.856[d]	19.3	22.8	$M1$		
		245	3^-	311.265[d,f]	6.8		$(E1)$		
		293	4^+	263.064[d]	4.5	4.6	$(M1+E2)$		
		314	2^-	242.314[d]	18.0	27.5	$M1+E2$		
		407	3^+	149.375[d]	7.0	8.0	$E1$		
561.855(5)[b]	5^+	147	4^+	414.783[d]	104.7	117.6	$M1$	136	0
		162	5^+	400.316[d]	5.8	6.6			
		271	3^+	290.913[d]	7.1	7.8	$(M1)$		
		407	3^+	154.853[d]	2.2	4.1			
578.490(4)[c]	3^-	147	4^+	431.526[d]	16.1	16.3	$E1$	95	0
		196	2^-	382.984[d]	17.6	20.2	$(M1+E2)$		
		377	3^-	201.506[d]	2.5	4.7			
		391	2^-	187.530[d]	8.4	17.4	$M1$		
		436	2^-	142.199[d]	11.1	36.7	$M1$		
579.146(2)[c]	2^-	82	1^-	496.818[d]	7.6	8.2	$E2$	380	90
		139	1^-	440.458[d]	37.5	41.5	$M1$		
		161	1^-	418.144[d]	103.6	116.1	$M1$		
		185	3^-	394.516[d]	7.3	8.3	$M1$		
		254	2^-	324.988[d]	50.2	61.9	$M1$		
		309	1^-	270.152[d]	3.8	5.2	$M1+E2$		
		314	2^-	265.093[d]	6.9	9.8	$M1$		
		391	2^-	188.175[d]	1.1	2.4			
		520	4^-	59.358[d]	2.6	126.4			
590.720(5)[c]	(3^+)	314	2^-	276.667[d]	5.8	6.0		17	35
		377	3^-	213.721[d]	10.2	10.8	$E1$		
599.403(5)[c]	2^-	112	2^-	487.176[d]	94.9	102.6	$M1$	188	8
		161	1^-	438.339[d]	5.0	5.5			
		245	3^-	354.289[d]	9.1	10.8	$M1$		
		254	2^-	345.237[d]	13.3	16.0	$M1$		
		279	2^-	320.844[d]	6.0	7.5	$M1+E2$		
		338	2^-	261.762[d]	3.7	5.3	$M1$		
		377	3^-	222.392[d]	3.6	6.1			
		391	2^-	208.443[d]	7.4	13.3	$M1$		
		436	2^-	163.120[d]	8.1	20.9	$M1$		

TABLE VI. (Continued.)

Level energy (keV)	Spin and parity	Pop. level (keV)	J^π pop. level	Trans. energy (keV)	γ int. (rel.)	Total int. (rel.)	Multi-pola-rity	Dep. int. (rel.)	Pop. int. (rel.)
605.531(4)[c]	3^-	0	1^-	605.762[d]	8.9	9.1	$M1$	164	0
		139	1^-	466.597[d]	23.3	24.0	$M1+E2$		
		161	1^-	444.699[d]	4.8	5.0			
		162	5^+	444.043[d]	11.0	14.6			
		185	3^-	420.846[d]	22.8	25.5	$M1$		
		245	3^-	360.423[d]	48.1	56.7	$M1+E2$		
		264	4^+	341.733[d]	9.8	9.9			
		377	3^-	228.518[d]	3.9	6.3	$M1$		
		424	2^-	181.799[d]	3.0	6.5	$M1$		
		436	2^-	169.214[d]	2.7	6.4			
613.089(5)[c]	$3, 4^-$	271	3^+	342.162[d]	10.8	11.0	$E1$	45	4
		293	4^+	319.850[d]	15.1	15.4	$E1$		
		297	4^-	316.423[d,f]	10.4		$E1$		
		361	4^+	251.695[d]	7.8	8.1	$E1$		
		520	4^+	93.562[d]	7.3	10.8	$E1$		
620.521(6)[h]	3^-	149	3^-	471.581[d]	34.5	37.5	$M1$	79	0
		185	3^-	435.840[d]	15.3	17.0	$M1+E2$		
		271	3^+	349.576[d]	6.5	6.6			
		579	2^-	41.416[d]	1.1	18.2			
638.773(3)[c]	$3, 4^-$	185	3^-	454.090[d]	15.2	16.7	$M1+E2$	68	0
		196	2^-	443.212[d]	6.7	7.0	$M1+E2$		
		297	4^-	342.162[d,f]	10.9		$E1$		
		377	3^-	261.762[d]	3.7	5.3	$M1$		
		420	3^-	219.163[d]	31.4	39.5	$E2$		
639.390(3)[c]	2^-	43	0^-	596.281[d]	8.2	8.3	$M1+E2$	169	0
		82	1^-	557.101[d]	25.7	27.1	$M1+E2$		
		112	2^-	527.178[d]	7.7	8.2	$M1$		
		139	1^-	500.664[d]	13.4	14.4	$M1+E2$		
		149	3^-	490.441[d]	8.4	9.0			
		161	1^-	478.388[d]	21.2	23.0	$M1$		
		245	3^-	394.329[d]	8.3	9.5			
		254	2^-	385.238[d]	10.8	12.4			
		309	1^-	330.418[d]	28.8	35.3	$M1$		
		338	1^-	301.877[d]	7.3	9.4			
		338	2^-	301.735[d]	3.8	4.9			
		490	2^-	149.777[d]	2.4	7.3			
646.534(9)[c]	4^+	147	4^+	499.456[d]	102.3	110.0	$E2+M1$	137	0
		361	4^+	285.146[d]	9.8	13.1	$M1+E2$		
		395	4^-	251.695[d]	7.8	8.1	$E1$		
		407	3^+	239.549[d]	4.0	6.2	$M1+E2$		
669.373(9)[c]	4^-	43	0^-	626.211[d,f]	19.6		$M1$	227	0
		112	2^-	557.101[d]	25.7	26.1	$M1+E2$		
		149	3^-	520.567[d,f]	28.8		$E1$		
		196	2^-	473.763[d]	5.7	5.9			
		245	3^-	424.323[d]	4.2	4.7			
		264	4^+	405.602[d]	17.5	17.7	$E2$		
		395	4^-	274.473[d]	5.1	7.0	$M1$		
		420	3^-	249.789[d,f]	6.5		$E1$		
		520	4^-	149.588[d]	3.1	9.2	$M1$		
		543	2^+	126.814[d]	6.5	156.8	$M1$		
670.121(6)[c]	3^-	112	2^-	558.074[d]	7.9	8.3		151	0
		139	1^-	531.388[d]	17.5	17.9	$M1$		
		149	3^-	521.191[d]	28.8	30.8	$E2$		
		279	2^-	391.497[d]	13.1	15.0	$E1$		
		377	3^-	293.123[d]	5.2	6.9	$M1$		

TABLE VI. *(Continued.)*

Level energy (keV)	Spin and parity	Pop. level (keV)	J^π pop. level	Trans. energy (keV)	γ int. (rel.)	Total int. (rel.)	Multi-pola-rity	Dep. int. (rel.)	Pop. int. (rel.)
		407	3^+	263.064[d]	4.5	4.6	$M1+E2$		
		420	3^-	250.526[d]	4.1	6.0			
		424	2^-	246.397[d]	5.8	8.7	$M1+E2$		
		520	4^-	150.348[d]	2.9	8.5			
		579	2^-	90.963[d]	4.7	44.1			
708.548(5)[c]	2^-	0	1^-	708.547[d]	92.9	95.9		334	0
		82	1^-	626.211[d]	19.5	20.3	$M1$		
		112	2^-	596.281[d]	8.2	8.6	$M1+E2$		
		144	0^-	565.016[d]	7.0	7.1	$M1$		
		161	1^-	547.558[d]	49.0	51.9	$M1$		
		196	2^-	513.017[d]	27.1	29.0	$M1+E2$		
		245	3^-	463.462[d]	8.0	8.8	$M1+E2$		
		279	2^-	430.053[d]	7.7	8.6	$M1+E2$		
		297	4^-	411.898[d]	21.3	22.1	$E1$		
		309	1^-	399.588[d]	12.7	14.5	$M1$		
		314	2^-	394.516[d]	7.3	8.3	$M1$		
		338	2^-	370.866[d]	6.5	7.6	$M1$		
		500	3^-	208.322[d]	8.3	14.9	$M1+E2$		
		545	2^-	163.896[d]	3.4	8.7	$M1$		
		579	2^-	129.312[d]	6.8	27.4	$M1$		
722.763(3)[c]	3^+	147	4^+	575.691[d]	46.8	49.3	$M1$	137	0
		185	3^-	538.030[d]	8.5	8.6			
		196	2^-	527.178[d]	7.7	7.8	$M1$		
		271	3^+	451.832[d]	8.9	9.8	$M1+E2$		
		279	2^-	444.250[d]	9.6	9.7			
		338	2^-	385.155[d]	8.3	8.4			
		486	2^-	236.777[d]	1.1	1.2			
		519	2^+	204.187[d]	15.1	27.8	$M1$		
		520	4^+	203.241[d]	3.2	5.9	$M1$		
		591	3^+	132.007[d]	2.2	8.6	$M1$		
738.343(5)[c]	4^+	84	2^-	653.928[d]	6.6	7.3		116	0
		162	5^+	576.819[d]	18.2	19.2			
		185	3^-	553.774[d]	7.7	7.7			
		271	3^+	467.413[d]	41.1	44.8	$M1$		
		314	2^-	424.323[d]	4.2	5.7			
		395	4^-	343.508[d]	4.8	4.9			
		417	4^-	321.681[d]	5.3	5.4	$M1+E2$		
		520	4^+	218.812[d]	5.7	9.6	$M1+E2$		
		545	2^-	193.685[d,f]	2.0		$M1$		
		591	3^+	147.630[d]	8.5	26.2	$M1+E2$		
		599	2^-	138.947[d,f]	8.2		$M1+E2$		
		613	4^-	125.221[d]	3.4	4.2			

[a]Depopulation intensities for these four levels below 200 keV are expected to be 20–30% higher than calculated from data; in all cases, underestimation of γ intensities for low-energy lines seems to be evident.
[b]New level compared with Ref. [1]. First observed in our $(\vec{d},\alpha)$ experiment.
[c]New level compared with Refs. [1,3].
[d]Newly placed γ from Ref. [1], or, for $E_\gamma > 500$ keV, from Tables IV and V.
[e]Spin-parity fixed compared with Ref. [1].
[f]These lines are not used for total intensity calculations.
[g]γ intensity for the 264.744 keV line (very probably a doublet) is divided into two equal parts.
[h]New level compared with Ref. [1]. First observed in our (d, p) experiment.

cases at higher energies. Comments on positive parity levels are more extensive, since the argumentation for these levels is more complex. A few spin-parity assignments are briefly discussed.

The confidence of the levels is not commented on level by level in Table VI. A use of different data sets could provide rather decisive arguments for the existence of a large part of the levels proposed in Table VI. Here, we comment on a few levels with higher (e.g., 245.5 or 590.7 keV) or lower (e.g., 639 keV) confidence than it may seem from a quick estimation.

147.1 keV 4^+: Now, spin 4 is beyond doubt, as well as the fact that it is the lowest positive parity level. Also, the lifetime of 32 ms is referred to this level. This lifetime was at first disclosed by Lundan and Siivola [24]. However, a reliable decay pattern of this isomeric state was found a bit later (see Ref. [1]).

148.9 keV $3^-(2^-)$: Spin 3 is preferred in Table VI, based on population-depopulation pattern. Spin 2 in Table I is probably influenced by the close 147.1 keV 4^+ level.

161.5 keV 5^+: This new level is proposed from the $(\vec{d},\alpha)$ reaction showing an angular distribution for spin-parity 5^+.

245.5 keV 0^-: This level has been evaluated as having a C confidence (i.e., being tentative) in the previous paper [1]. Additional analysis allows confidence B (i.e., being rather certain).

263.8, 293.2, and 361.4 keV, levels with positive parity: They can have B confidence because of a lack of direct observations.

270.9 keV 3^+: Since this level is connected by an $E2$ transition to the 161.5 keV 5^+ level and the $(\vec{d},\alpha)$ data indicate the possibilities 2^- and 3^+, the 3^+ assignment seems to be a better choice if compared with an earlier model-independent $3^+, 4^+$ assignment. In analyzing the rotational band structure, spin values 270.9 keV 3^+ and 519.5 keV 4^+ are important for a probable nuclear shape change (see below).

391.0 keV 2^-: Spin-parity is fixed compared with that in Ref. [1]. Spin value 2 is strongly favored by the two most intense depopulating transitions. Alternative value 3 has come from intensity in the ARC spectra [1]; however, corresponding intensity errors (less than 10%) seem to be underestimated.

394.9 keV 4^-: The $(\vec{d},\alpha)$ data suggest a $3^+, 4^-$ level at 393.3 keV. However, energy and intensity of this level seem to be influenced by the nearby 391.0 keV 2^- level. Therefore, we propose a new 4^- level at 394.9 keV. Depopulating transitions to the lower 2^- levels at 84.3 and 112.2 keV are examples where transition multipolarities were not exactly estimated in the earlier evaluation, since the intensity errors are larger than quoted. Both 4^- to 2^- transitions can be pure $E2$.

416.6 keV 4^-: This is a new level first seen in $(\vec{d},\alpha)$. Spin and parity 4^- agree with all essential arguments: decay transitions and their multipolarities, quantum numbers favored by the $(\vec{d},\alpha)$ data, and a lack of high-energy transitions from neutron capture.

467.2 keV 4^-: Spin-parity is fixed compared with that in Ref. [1]. Although four probable depopulating transitions are included in Table IV to spin 0, 1 levels, their "quality" (energy errors, intensity) is clearly weaker than for those to spin 2–5 levels. Analysis of the decay pattern is favorable for spin 4 of this level. In neutron capture high-energy spectra, no transition is observed.

486.1 keV 2^-: A new 486.1 keV level is given in the neighborhood of the 489.6 keV level. These levels form a doublet that is partially resolved in the (d, p) reaction spectra. The 489.6 keV level has spin-parity 2^-.

561.9 keV 5^+: The intense transition to the 147.1 keV 4^+ level and the $(\vec{d},\alpha)$ data imply the spin assignment of the 561.9 keV level, although multipolarities of weaker depopulating transitions would also allow smaller spin values, such as 3 or 4.

578.5 keV 3^- *and* 579.1 *keV* 2^-: These two levels form a doublet with negative parity clearly supported both by the ARC data and primary thermal neutron capture γ spectrum. Also the (d, p) data support at least one of these levels.

590.7 keV (3^+), 2^-: In an "underdeveloped" positive parity system of ^{194}Ir, such a tentative level is of interest, since up-to-now unknown positive parity levels can enable us to find appropriate connecting transitions. In Table I, the assignment is 2^-, but a level with such spin-parity does not fit into the (n,γ) scheme. A doublet of levels within a few keV could not be found as well. However, the existence of a level near this energy is suggested by our data (Table I).

620.5 keV: This is the only level where the spin assignments of (n,γ) and (d,α) are in contradiction (cf. Table I). There may be a close doublet.

639 keV: From the two levels of a doublet, at 638.7 and 639.4 keV, the former level is less certain, since it has a smaller number of well-defined connecting transitions.

646 keV: This level is somewhat tentative because of the lack of direct observations.

669 and 670 keV: A limited number of transitions with small energy errors does not allow us to have the best confidence for these levels.

722.8 keV 3^+: The level is supported by reliable energy combinations of transitions to lower levels, and a lack of observations in any direct reaction does not seriously decrease its confidence.

738.3 keV 4^+: This level is also only based on transition energies and multipolarities; however, the decay pattern, including end-level spins-parities, is as expected.

IV. THEORETICAL MODELS

A. Nilsson model

In the ^{194}Ir level structure study, interpretation via Nilsson orbits in the axially symmetric weakly deformed field has already been attempted [1]. Associated rotational bands were developed on a basis of existing data. Twelve rotational bands and/or bandheads were defined.

We try to include corrections into the earlier version of this type of model interpretation. Although the basis has been used earlier and the number of rotational bands is about the same, we believe that the revised interpretation is essentially better, as shown in Table VII.

TABLE VII. Bandheads and rotational levels assigned in ^{194}Ir. Energies from Table VI.

K^π	I^π	E(keV)	K^π	I^π	E(keV)
1^-	1^-	0.0	0^-	0^-	245.5
	2^-	84.3		1^-	337.5
	3^-	184.7		2^-	337.6
	4^-	296.6	2^-	2^-	278.5
1^-	1^-	138.7		3^-	347.1
	2^-	254.2	2^-	2^-	391.0
	3^-	419.6		3^-	578.5
1^-	1^-	161.0	3^-	3^-	148.9
	2^-	314.1		4^-	394.9
	3^-	500.2	11^-	11^-	240–440
0^-	0^-	43.1	2^+	2^+	518.6
	1^-	82.3		3^+	722.8
	2^-	112.2	3^+	3^+	270.9
	3^-	245.1		4^+	519.5
0^-	0^-	143.6	4^+	4^+	147.1
	1^-	309.0		5^+	561.9
	2^-	195.5	5^+	5^+	161.5

The exact formulation with which Nilsson orbits are used for the proton number $Z = 77$ and neutron number $N = 117$ should help derive the corresponding two-particle configurations. The basis used previously is the following: for protons, $3/2^+[402]$, $1/2^+[400]$, $11/2^-[505]$; for neutrons, $3/2^-[512]$, $1/2^-[510]$, $11/2^+[615]$. It is presented previously in Ref. [1] (see Tables 9 and 10 as well as corresponding discussion in the cited paper), and it has been assumed that rather strongly mixed bands have dominating components. We expect 18 bands. Nine negative parity bands with K values between 0 and 3 should exist, and one band $K = 11^-$: three bands $K = 0$, three bands $K = 1$, two bands $K = 2$, and one band $K = 3$. Eight positive parity bands with K between 4 and 7 are expected. Since higher spins are required for their observation, those with $K = 6$ or $K = 7$ could not be identified.

An important new result is the addition of new rotational band members. From our viewpoint, several of the proposed rotational bands deserve comments. To repeat the idea that bands with the same parity and K value are strongly mixed [1], we discuss negative parity bands with $K = 1$ (starting with the ground state band), with $K = 0$, $K = 2$, $K = 3$, and $K = 11$, and the positive parity bands.

It seems strange that the 1^- ground state band is developed only up to 3^- (184.7 keV). Probably, the 296.6 keV level is $K = 1$, not $K = 0$ from the previous assignment. Considering transition intensities, the strongest depopulation of this level is to the 84.2 keV 2^- level with $K = 1$. The intensity is 34, and the total depopulation from the 296.6 keV level is 67 (see Table VI).

Although higher negative parity bands with low K values are more problematic, a traditional approach to searching for transitions inside bands gives new results: $J = 3$ band members in the 161.0 keV 1^- band and 391.0 keV 2^- band are good examples. A tentative solution is the construction of the 278.5 keV 2^- band. The decay of the 347.1 keV level can be obscured by x-ray lines. The high irregularity of the $K = 0$ bands is an obstacle to their extension to higher spins. The $K = 3^-$ band with the bandhead at 148.9 keV could be continued with the 394.9 keV 4^- level, having both a "rotational" transition and an $E2$ transition to the 84.3 keV 2^- level. The latter transition is similar in structure change and multipolarity to the 148.9 keV $E2$ transition from the 3^- bandhead to the 1^- ground state.

For a complete picture of ^{194}Ir, the long-lived isomer with $T_{(1/2)} = 161$ yr [3,25] should be mentioned here. However, the energy of this level is poorly known; it is expected to be in the energy range 240–440 keV. The observation of the level via β decay, and its spin-parity 11^-, are well established. The problem of the incorrect energy arises, since a γ-depopulation is not observed. An appropriate bandhead is expected via $\Omega_p = \Omega_n = 11/2$.

The 147.1 keV 4^+ level had been a lonely band head earlier. Because of a "rotational" transition having intensity as expected, the 561.9 keV 5^+ level is proposed as a second member. A rotational parameter value of $A = 41.5$ keV is probably acceptable.

The 270.9 keV 3^+ level forms a two-member rotational band with the 519.5 keV 4^+ level, and $A = 31$ keV. Its structure cannot be explained.

The 518.6 keV 2^+ level is supposed to be a bandhead with the 3^+ member at 722.7 keV. This level depopulates to the 147.1 keV 4^+ and 518.6 keV 2^+ levels. A depopulation to the 561.9 keV 5^+ level is possible; however, it is obscured by the strong γ lines 160.8 and 160.9 keV.

B. Nuclear supersymmetry

1. Level scheme

Dynamical supersymmetry (SUSY) was introduced [26] in nuclear physics in the context of the interacting boson model (IBM) and its extensions. The IBM describes collective excitations in even-even nuclei in terms of a system of interacting monopole ($s^\dagger$) and quadrupole ($d^\dagger$) bosons, which altogether can be denoted by $b_i^\dagger$ with angular momentum $l = 0, 2$. The bosons are associated with the number of correlated proton and neutron pairs, and hence the number of bosons N is half the number of valence nucleons [27].

For odd-mass nuclei, the IBM was extended to include single-particle degrees of freedom [28]. The ensuing interacting boson-fermion model (IBFM) has as its building blocks N bosons with $l = 0, 2$ and $M = 1$ fermion ($a_j^\dagger$) with $j = j_1, j_2, \ldots$ [29]. The IBM and IBFM can be unified into a supersymmetry (SUSY) [30]

$$U(6/\Omega) \supset U(6) \otimes U(\Omega), \quad (3)$$

where $\Omega = \sum_j (2j + 1)$ is the dimension of the fermion space. In this framework, even-even and odd-even nuclei form the members of a supermultiplet, which is characterized by $\mathcal{N} = N + M$, i.e., the total number of bosons and fermions. Supersymmetry distinguishes itself from other symmetries in that it includes, in addition to transformations among fermions and among bosons, transformations that change a boson into a fermion and vice versa.

Dynamical nuclear supersymmetries correspond to very special forms of the Hamiltonian which may not be applicable to all regions of the nuclear chart, but nevertheless many nuclei have been found to provide experimental evidence for supersymmetries in nuclei [29,31]. Especially, the mass region $A \sim 190$ has been a rich source of empirical evidence for the existence of (super)symmetries in nuclei. The even-even nucleus ^{196}Pt is the standard example of the SO(6) limit of the IBM [32]. The odd-proton nuclei ^{191,193}Ir and ^{193,195}Au were suggested as examples of the Spin(6) limit [26], in which the odd proton is allowed to occupy the $2d_{3/2}$ orbit of the 50–82 proton shell, whereas the pairs of nuclei ^{190}Os-^{191}Ir, ^{192}Os-^{193}Ir, ^{192}Pt-^{193}Au, and ^{194}Pt-^{195}Au have been analyzed as examples of a U(6/4) SUSY [30].

The odd-neutron nucleus ^{195}Pt, together with ^{194}Pt, was studied in terms of a U(6/12) SUSY [33], in which the odd neutron occupies the $3p_{1/2}$, $3p_{3/2}$, and $2f_{5/2}$ orbits of the 82–126 neutron shell. In this case, the neutron angular momenta are decoupled into a pseudo-orbital part with $\tilde{l} = 0, 2$ and a pseudospin part with $\tilde{s} = \frac{1}{2}$. This SUSY scheme arises from the equivalence between the values of the angular momenta of the pseudo-orbital part and those of the bosons of the IBM.

The concept of nuclear SUSY was extended in 1985 to include the neutron-proton degree of freedom [34]. In this case, a supermultiplet consists of an even-even, an odd-proton, an odd-neutron, and an odd-odd nucleus. At present, the best experimental evidence of a supersymmetric quartet is provided by the ^{194,195}Pt and ^{195,196}Au nuclei as an example of the $U_\nu(6/12)\otimes U_\pi(6/4)$ SUSY [22,35,36]. This supermultiplet is characterized by $\mathcal{N}_\pi = 2$ and $\mathcal{N}_\nu = 5$. The excitation spectra of the nuclei belonging to the supersymmetric quartet are described simultaneously by the energy formula

$$\begin{aligned} E = {} & A[N_1(N_1+5) + N_2(N_2+3) + N_1(N_1+1)] \\ & + B\big[\Sigma_1(\Sigma_1+4) + \Sigma_2(\Sigma_2+2) + \Sigma_3^2\big] \\ & + B'\big[\sigma_1(\sigma_1+4) + \sigma_2(\sigma_2+2) + \sigma_3^2\big] \\ & + C[\tau_1(\tau_1+3) + \tau_2(\tau_2+1)] \\ & + DL(L+1) + EJ(J+1). \end{aligned} \tag{4}$$

The coefficients A, B, B', C, D, and E can be determined in a simultaneous fit of the excitation energies of the four nuclei that make up the quartet. J is in this case the integer quantum number; L the half-integer.

Another quartet of nuclei that has been studied in some detail as a possible example of the $U(6/12)_\nu\otimes U(6/4)_\pi$ supersymmetry is provided by the nuclei ^{192,193}Os and ^{193,194}Ir [4,37]. The difference with the previously mentioned quartet of ^{194,195}Pt and ^{195,196}Au nuclei is in the number of protons; the number of neutrons is the same. Since the valence protons are holelike, this supermultiplet is characterized by $\mathcal{N}_\pi = 3$ and $\mathcal{N}_\nu = 5$. This expectation is based on the fact that the pair ^{192}Os-^{193}Ir is considered to be a good example of U(6/4) [30,38]. In comparison with the Pt-Au quartet, the odd-neutron nucleus ^{193}Os is much less well-known experimentally than ^{195}Pt, which is considered to be the best example of U(6/12). The main coupling between the odd neutron and the core nucleus is of quadrupole type. It has been shown [39] that the quadrupole-quadrupole interaction of U(6/12) arises from the more general form used in the IBFM for very special choices of the occupation probabilities of the $3p_{1/2}$, $3p_{3/2}$, and $2f_{5/2}$ orbits, i.e., to the location of the Fermi surface for the neutron orbits. This situation is to a good approximation satisfied by the nucleus ^{195}Pt. Since the number of neutrons in the pair of nuclei ^{192}Os-^{193}Os is the same as that for ^{194}Pt-^{194}Pt, it is expected that this condition also holds for the ^{193}Os nucleus. For this reason, the pair of nuclei ^{192,193}Os is expected to provide a good example of U(6/12). In the same vein, the odd-odd nucleus ^{194}Ir which completes the quartet is expected, just as ^{196}Au, to be a good example of $U(6/12)_\nu\otimes U(6/4)_\pi$ supersymmetry.

The negative parity levels in the odd-odd nucleus ^{194}Ir were studied in the supersymmetric scheme for the first time in 1996 [4]. The implicit assumption is made that the states of negative parity occurring at low-excitation energy in the experimental spectrum originate only from the $(\nu 3p_{1/2}, \nu 3p_{3/2}, \nu 2f_{5/2}) \otimes \pi 2d_{3/2}$ configurations. The ground state was reproduced correctly, and the number of states with a certain spin corresponded roughly to the experimental situation. The density of theoretical levels above 400 keV was greater than observed, but this could be related to the fact that these levels might not have been observed yet experimentally. A comparison of one-nucleon transfer data in Ref. [4] showed that whereas the results for the $l = 1$ strength were quite good, SUSY overpredicted the $l = 3$ strength. The latter might be due to missing experimental strength.

On the basis of the new spectroscopic information presented in this article and especially the analysis of the two-nucleon transfer reaction ^{196}Pt$(\vec{d}, \alpha)^{194}$Ir in the supersymmetry scheme, we have made new assignments for the negative parity low-lying experimental levels to obtain a much improved description of the nuclear structure of ^{194}Ir (see Table VIII). The main change is that the ground state of ^{194}Ir is assigned to the band $[N+1, 0]$, $\langle N+\frac{3}{2}, \frac{1}{2}, \frac{1}{2}\rangle$ instead of to $[N, 1]$, $\langle N+\frac{1}{2}, \frac{1}{2}, -\frac{1}{2}\rangle$ as in Ref. [4]. Here N is the number of bosons in the odd-odd nucleus ($N = 6$ for ^{194}Ir). The new assignment agrees with that of the neighboring odd-odd nucleus ^{196}Au [22,35,36]. The energy spectrum of ^{194}Ir is calculated using the energy formula of Eq. (4) with $A = 26.3$, $B = 8.7$, $B' = -33.6$, $C = 35.1$, $D = 6.3$, and $E = 4.5$ (all in keV). The values of these parameters are a lot closer to the values used for ^{196}Au indicating systematics in this zone of the nuclear chart. Figure 4 shows a comparison between the theoretical spectrum and the experimental level scheme. A one-to-one correspondence results for the 23 lowest lying theoretical states, and the structure of the experimental level scheme is very well reproduced by the extended SUSY when it is employed in its most basic form, i.e., a dynamical SUSY.

TABLE VIII. SUSY assignments for the negative parity low-lying levels in ^{194}Ir. $R^{(1)}_{\mathrm{LJ}}$ and $R^{(2)}_{\mathrm{LJ}}$ refer to the normalized transitions strengths of Table I. Theoretical states with $\tau_1 = 5/2$ have strength zero because they are outside the model space. The nearly one-to-one correspondence of the level schemes can be seen in Fig. 4. The transfer strengths are visualized in Fig. 5.

Experiment			Theory					
E [keV]	J^π	$R^{(1)}_{\mathrm{LJ}}/R^{(2)}_{\mathrm{LJ}}$	$[N_1, N_2]$	$\langle\Sigma_1, \Sigma_2\rangle$	$\langle\sigma_1, \sigma_2, \sigma_3\rangle(\tau_1, \tau_2)L$	J^π	E[keV]	$R^{(1)}_{\mathrm{LJ}}/R^{(2)}_{\mathrm{LJ}}$
0.0	1^-	0.5 / –	[7, 0]	$\langle 7, 0\rangle$	$\langle\tfrac{15}{2}, \tfrac{1}{2}, \tfrac{1}{2}\rangle(\tfrac{1}{2}, \tfrac{1}{2})\tfrac{3}{2}$	1^-	0.0	0.7 / –
43.1	0^-	1.0 / –	[6, 1]	$\langle 6, 1\rangle$	$\langle\tfrac{13}{2}, \tfrac{3}{2}, \tfrac{1}{2}\rangle(\tfrac{3}{2}, \tfrac{1}{2})\tfrac{1}{2}$	0^-	126.9	1.0 / –
82.3	1^-		[6, 1]	$\langle 6, 1\rangle$	$\langle\tfrac{13}{2}, \tfrac{1}{2}, -\tfrac{1}{2}\rangle(\tfrac{1}{2}, \tfrac{1}{2})\tfrac{3}{2}$	1^-	113.8	0.2 / –
84.3	2^-	0.2 / 1.0	[7, 0]	$\langle 7, 0\rangle$	$\langle\tfrac{15}{2}, \tfrac{1}{2}, \tfrac{1}{2}\rangle(\tfrac{1}{2}, \tfrac{1}{2})\tfrac{3}{2}$	2^-	18.0	0.4 / 1.0
112.2	2^-	0.3 / 0.4	[6, 1]	$\langle 6, 1\rangle$	$\langle\tfrac{13}{2}, \tfrac{1}{2}, -\tfrac{1}{2}\rangle(\tfrac{1}{2}, \tfrac{1}{2})\tfrac{3}{2}$	2^-	131.8	0.2 / 0.1
138.7	1^-	1.0 / –	[6, 1]	$\langle 6, 1\rangle$	$\langle\tfrac{13}{2}, \tfrac{3}{2}, \tfrac{1}{2}\rangle(\tfrac{3}{2}, \tfrac{1}{2})\tfrac{1}{2}$	1^-	135.9	1.0 / –
143.6	0^-		[7, 0]	$\langle 7, 0\rangle$	$\langle\tfrac{15}{2}, \tfrac{1}{2}, \tfrac{1}{2}\rangle(\tfrac{3}{2}, \tfrac{1}{2})\tfrac{1}{2}$	0^-	147.4	0.3 / –
148.9	3^-	0.3 / –	[6, 1]	$\langle 6, 1\rangle$	$\langle\tfrac{13}{2}, \tfrac{3}{2}, \tfrac{1}{2}\rangle(\tfrac{3}{2}, \tfrac{1}{2})\tfrac{5}{2}$	3^-	231.5	0.2 / –
161.0	1^-		[7, 0]	$\langle 7, 0\rangle$	$\langle\tfrac{15}{2}, \tfrac{1}{2}, \tfrac{1}{2}\rangle(\tfrac{3}{2}, \tfrac{1}{2})\tfrac{1}{2}$	1^-	156.4	0.3 / –
184.7	3^-		[7, 0]	$\langle 7, 0\rangle$	$\langle\tfrac{15}{2}, \tfrac{1}{2}, \tfrac{1}{2}\rangle(\tfrac{3}{2}, \tfrac{1}{2})\tfrac{5}{2}$	3^-	251.9	0.1 / –
195.5	2^-	0.1 / 0.3	[7, 0]	$\langle 7, 0\rangle$	$\langle\tfrac{15}{2}, \tfrac{1}{2}, \tfrac{1}{2}\rangle(\tfrac{3}{2}, \tfrac{1}{2})\tfrac{5}{2}$	2^-	224.9	0.3 / 0.0
245.1	3^-		[6, 1]	$\langle 6, 1\rangle$	$\langle\tfrac{13}{2}, \tfrac{3}{2}, \tfrac{1}{2}\rangle(\tfrac{3}{2}, \tfrac{3}{2})\tfrac{5}{2}$	3^-	336.7	0.0 / –
245.5	0^-		[6, 1]	$\langle 6, 1\rangle$	$\langle\tfrac{13}{2}, \tfrac{1}{2}, -\tfrac{1}{2}\rangle(\tfrac{3}{2}, \tfrac{1}{2})\tfrac{1}{2}$	0^-	261.2	0.1 / –
254.2	2^-	1.0 / 0.0	[6, 1]	$\langle 6, 1\rangle$	$\langle\tfrac{13}{2}, \tfrac{3}{2}, \tfrac{1}{2}\rangle(\tfrac{3}{2}, \tfrac{1}{2})\tfrac{5}{2}$	2^-	204.5	1.0 / 0.0
278.5	2^-		[6, 1]	$\langle 6, 1\rangle$	$\langle\tfrac{13}{2}, \tfrac{3}{2}, \tfrac{1}{2}\rangle(\tfrac{3}{2}, \tfrac{3}{2})\tfrac{3}{2}$	2^-	278.1	0.0 / 0.0
296.6	4^-	0.8 / 0.9	[6, 1]	$\langle 6, 1\rangle$	$\langle\tfrac{13}{2}, \tfrac{3}{2}, \tfrac{1}{2}\rangle(\tfrac{3}{2}, \tfrac{1}{2})\tfrac{7}{2}$	4^-	311.7	1.0 / 1.0
309.0	1^-		[6, 1]	$\langle 6, 1\rangle$	$\langle\tfrac{13}{2}, \tfrac{3}{2}, \tfrac{1}{2}\rangle(\tfrac{3}{2}, \tfrac{3}{2})\tfrac{3}{2}$	1^-	260.1	0.0 / –
314.1	2^-	0.2 / 0.1	[6, 1]	$\langle 6, 1\rangle$	$\langle\tfrac{13}{2}, \tfrac{1}{2}, -\tfrac{1}{2}\rangle(\tfrac{3}{2}, \tfrac{1}{2})\tfrac{5}{2}$	2^-	338.7	0.1 / 0.0
337.5	1^-		[6, 1]	$\langle 6, 1\rangle$	$\langle\tfrac{13}{2}, \tfrac{1}{2}, -\tfrac{1}{2}\rangle(\tfrac{3}{2}, \tfrac{1}{2})\tfrac{1}{2}$	1^-	270.2	0.1 / –
337.6	2^-	0.0 / 0.1	[6, 1]	$\langle 6, 1\rangle$	$\langle\tfrac{13}{2}, \tfrac{3}{2}, \tfrac{1}{2}\rangle(\tfrac{3}{2}, \tfrac{3}{2})\tfrac{5}{2}$	2^-	309.7	0.0 / 0.0
347.1	3^-	1.0 / –	[6, 1]	$\langle 6, 1\rangle$	$\langle\tfrac{13}{2}, \tfrac{3}{2}, \tfrac{1}{2}\rangle(\tfrac{3}{2}, \tfrac{1}{2})\tfrac{7}{2}$	3^-	275.7	1.0 / –
377.0	3^-		[7, 0]	$\langle 7, 0\rangle$	$\langle\tfrac{15}{2}, \tfrac{1}{2}, \tfrac{1}{2}\rangle(\tfrac{3}{2}, \tfrac{1}{2})\tfrac{7}{2}$	3^-	296.1	0.3 / –
391.0	2^-		[6, 1]	$\langle 6, 1\rangle$	$\langle\tfrac{13}{2}, \tfrac{3}{2}, \tfrac{1}{2}\rangle(\tfrac{5}{2}, \tfrac{1}{2})\tfrac{3}{2}$	2^-	418.3	0.0 / 0.0
394.9	4^-	0.4 / 1.0	[7, 0]	$\langle 7, 0\rangle$	$\langle\tfrac{15}{2}, \tfrac{1}{2}, \tfrac{1}{2}\rangle(\tfrac{3}{2}, \tfrac{1}{2})\tfrac{7}{2}$	4^-	332.1	0.3 / 0.3
			[6, 1]	$\langle 6, 1\rangle$	$\langle\tfrac{13}{2}, \tfrac{3}{2}, \tfrac{1}{2}\rangle(\tfrac{5}{2}, \tfrac{1}{2})\tfrac{3}{2}$	1^-	400.3	0.0 / –
			[6, 1]	$\langle 6, 1\rangle$	$\langle\tfrac{13}{2}, \tfrac{1}{2}, -\tfrac{1}{2}\rangle(\tfrac{3}{2}, \tfrac{1}{2})\tfrac{7}{2}$	3^-	409.9	0.1 / –
416.6	4^-	1.0 / 0.1	[6, 1]	$\langle 6, 1\rangle$	$\langle\tfrac{13}{2}, \tfrac{1}{2}, -\tfrac{1}{2}\rangle(\tfrac{3}{2}, \tfrac{1}{2})\tfrac{7}{2}$	4^-	445.9	0.1 / 0.1
419.6	3^-		[6, 1]	$\langle 6, 1\rangle$	$\langle\tfrac{13}{2}, \tfrac{1}{2}, -\tfrac{1}{2}\rangle(\tfrac{3}{2}, \tfrac{1}{2})\tfrac{5}{2}$	3^-	365.7	0.0 / –
			[7, 0]	$\langle 7, 0\rangle$	$\langle\tfrac{15}{2}, \tfrac{1}{2}, \tfrac{1}{2}\rangle(\tfrac{5}{2}, \tfrac{1}{2})\tfrac{3}{2}$	1^-	420.7	0.0 / –
423.7	2^-		[7, 0]	$\langle 7, 0\rangle$	$\langle\tfrac{15}{2}, \tfrac{1}{2}, \tfrac{1}{2}\rangle(\tfrac{5}{2}, \tfrac{1}{2})\tfrac{3}{2}$	2^-	438.7	0.0 / 0.0
436.3	2^-	0.8 / 0.0	[6, 1]	$\langle 6, 1\rangle$	$\langle\tfrac{13}{2}, \tfrac{3}{2}, \tfrac{1}{2}\rangle(\tfrac{5}{2}, \tfrac{1}{2})\tfrac{5}{2}$	2^-	449.9	0.0 / 0.0
467.2	4^-		[6, 1]	$\langle 6, 1\rangle$	$\langle\tfrac{13}{2}, \tfrac{3}{2}, \tfrac{1}{2}\rangle(\tfrac{3}{2}, \tfrac{3}{2})\tfrac{9}{2}$	4^-	473.7	0.0 / 0.0
			[6, 1]	$\langle 6, 1\rangle$	$\langle\tfrac{13}{2}, \tfrac{3}{2}, \tfrac{1}{2}\rangle(\tfrac{5}{2}, \tfrac{1}{2})\tfrac{5}{2}$	3^-	476.9	0.0 / –
			[6, 1]	$\langle 6, 1\rangle$	$\langle\tfrac{13}{2}, \tfrac{3}{2}, \tfrac{1}{2}\rangle(\tfrac{5}{2}, \tfrac{3}{2})\tfrac{1}{2}$	0^-	477.6[a]	0.0 / –
486.1	2^-		[7, 0]	$\langle 7, 0\rangle$	$\langle\tfrac{15}{2}, \tfrac{1}{2}, \tfrac{1}{2}\rangle(\tfrac{5}{2}, \tfrac{1}{2})\tfrac{5}{2}$	2^-	470.3	0.0 / 0.0
			[6, 1]	$\langle 6, 1\rangle$	$\langle\tfrac{13}{2}, \tfrac{3}{2}, \tfrac{1}{2}\rangle(\tfrac{5}{2}, \tfrac{3}{2})\tfrac{1}{2}$	1^-	486.6[a]	0.0 / –
489.6	2^-	0.5 / 0.4	[6, 1]	$\langle 6, 1\rangle$	$\langle\tfrac{11}{2}, \tfrac{1}{2}, \tfrac{1}{2}\rangle(\tfrac{1}{2}, \tfrac{1}{2})\tfrac{3}{2}$	2^-	512.2[a]	0.1 / 0.3
			[6, 1]	$\langle 6, 1\rangle$	$\langle\tfrac{11}{2}, \tfrac{1}{2}, \tfrac{1}{2}\rangle(\tfrac{1}{2}, \tfrac{1}{2})\tfrac{3}{2}$	1^-	494.2[a]	0.0 / –
			[7, 0]	$\langle 7, 0\rangle$	$\langle\tfrac{15}{2}, \tfrac{1}{2}, \tfrac{1}{2}\rangle(\tfrac{5}{2}, \tfrac{1}{2})\tfrac{5}{2}$	3^-	497.3	0.0 / –
			[6, 1]	$\langle 6, 1\rangle$	$\langle\tfrac{13}{2}, \tfrac{3}{2}, \tfrac{1}{2}\rangle(\tfrac{5}{2}, \tfrac{3}{2})\tfrac{3}{2}$	1^-	505.5[a]	0.0 / 0.0

[a]These theoretical levels are not shown in Fig. 4.

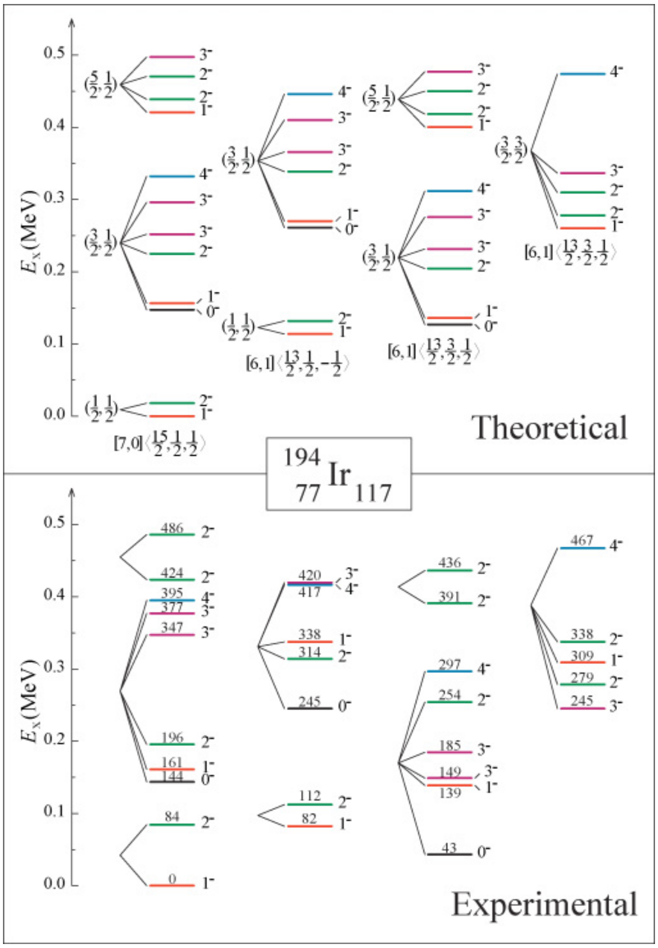

FIG. 4. (Color online) Comparison between the theoretical and experimental spectrum of ^{194}Ir. All experimental negative parity states below 486 keV are shown. A nearly one-to-one correlation between the experimental and the calculated level scheme is supported by $(\vec{d},\alpha)$ transfer strengths (see Sec. IV B2). The experimental levels at 395, 417, and 486 keV are first reported in this publication.

2. Two-nucleon transfer reactions

Two-nucleon transfer reactions probe the structure of the final nucleus through the exploration of two-nucleon correlations that may be present. The spectroscopic strengths not only depend on the similarity between the states in the initial and final nucleus, but also on the correlation of the transferred pair of nucleons.

In this section, the data on the ^{196}Pt$(\vec{d},\alpha)^{194}$Ir reaction are compared with the predictions from the $U_\nu(6/12)\otimes U_\pi(6/4)$ supersymmetry. This reaction involves the transfer of a proton-neutron pair, and hence measures the neutron-proton correlation in the odd-odd nucleus. The spectroscopic strengths $G_{\rm LJ}$

$$G_{\rm LJ}=\left|\sum_{j_\nu j_\pi} g^{\rm LJ}_{j_\nu j_\pi}\langle ^{194}{\rm Ir}\|\left(a^\dagger_{j_\nu}a^\dagger_{j_\pi}\right)^{(\lambda)}\|^{196}{\rm Pt}\rangle\right|^2, \tag{5}$$

TABLE IX. Tensorial character of the two-nucleon transfer operator.

Tensor	$(\sigma_1,\sigma_2,\sigma_3)$	(τ_1,τ_2)
T_1	$(\frac{1}{2},\frac{1}{2},-\frac{1}{2})$	$(\frac{1}{2},\frac{1}{2})$
T_2	$(\frac{3}{2},\frac{1}{2},\frac{1}{2})$	$(\frac{1}{2},\frac{1}{2})$
T_3	$(\frac{3}{2},\frac{1}{2},\frac{1}{2})$	$(\frac{3}{2},\frac{1}{2})$

depend on the reaction mechanism via the coefficients $g^{\rm LJ}_{j_\nu j_\pi}$ and on the nuclear structure part via the reduced matrix elements [5].

The transfer operator in Eq. (5) can be expanded in terms of three tensor operators under Spin(6) and Spin(5) (see Table IX) [5]. Since the ground state of ^{196}Pt has $(\tau_1,\tau_2)=(0,0)$, the only states in ^{194}Ir that can be excited are those with $(\tau_1,\tau_2)=(\frac{1}{2},\frac{1}{2})$ or $(\frac{3}{2},\frac{1}{2})$. The former can be populated by either T_1 or T_2, whereas the latter only by T_3.

To compare with experimental data, we calculate the relative strengths $R_{\rm LJ}=G_{\rm LJ}/G^{\rm ref}_{\rm LJ}$, where $G^{\rm ref}_{\rm LJ}$ is the spectroscopic strength of a reference state. The ratios of spectroscopic strengths to final states with $(\tau_1,\tau_2)=(\frac{3}{2},\frac{1}{2})$ provide a direct test of the nuclear wave functions, since they can only be excited by the tensor operator T_3 [5]. In Table X, we show the ratios for different states with $(\tau_1,\tau_2)=(\frac{3}{2},\frac{1}{2})$. The last column shows the numerical value relevant for the two-nucleon transfer reaction ^{196}Pt$(\vec{d},\alpha)^{194}$Ir ($N=6$).

Table VIII and Fig. 5 show a remarkable agreement between the theoretical predictions from nuclear SUSY and the two-nucleon transfer data for ratios of spectroscopic strengths $R_{\rm LJ}$. The reference states are easily identified, since they are normalized to unity. Here we emphasize that the calculations were carried out without the introduction of any new parameter. The coefficients $g^{\rm LJ}_{j_\nu j_\pi}$ appearing in the transfer operator of Eq. (5) were taken from the study of the ^{198}Hg$(\vec{d},\alpha)^{196}$Au reaction [5]. The deviations observed in the P_2 and F_2 transfers are most likely due to single-particle configurations outside the model space. For the P_0, P_1, and F_3 distributions, the experimental $(\vec{d},\alpha)$ detection limits for weakly populated 0^-, 1^-, and 3^- states prevent a better agreement.

TABLE X. Ratios of spectroscopic strengths. N is the number of bosons in the odd-odd nucleus, $\Sigma_3=0$. The last column shows the predictions for ^{194}Ir ($N=6$).

$[N_1,N_2]$	(Σ_1,Σ_2)	$(\sigma_1,\sigma_2,\sigma_3)$	$R_{\rm LJ}$	$N=6$
$[N,1]$	$(N,1)$	$(N+\frac{1}{2},\frac{3}{2},\frac{1}{2})$	1	1
$[N,1]$	$(N,1)$	$(N+\frac{1}{2},\frac{1}{2},-\frac{1}{2})$	$\frac{N+4}{15N}$	0.111
$[N,1]$	$(N,1)$	$(N-\frac{1}{2},\frac{3}{2},-\frac{1}{2})$	$\frac{(N+4)(N+1)(N-1)}{N(N+3)(N+5)}$	0.589
$[N,1]$	$(N,1)$	$(N-\frac{1}{2},\frac{1}{2},\frac{1}{2})$	$\frac{(N+1)(N-1)}{15(N+3)(N+5)}$	0.024
$[N+1,0]$	$(N+1,0)$	$(N+\frac{3}{2},\frac{1}{2},\frac{1}{2})$	$\frac{2(N+4)(N+6)}{15N(N+3)}$	0.296
$[N+1,0]$	$(N+1,0)$	$(N+\frac{1}{2},\frac{1}{2},-\frac{1}{2})$	$\frac{2(N+4)}{15(N+3)}$	0.148

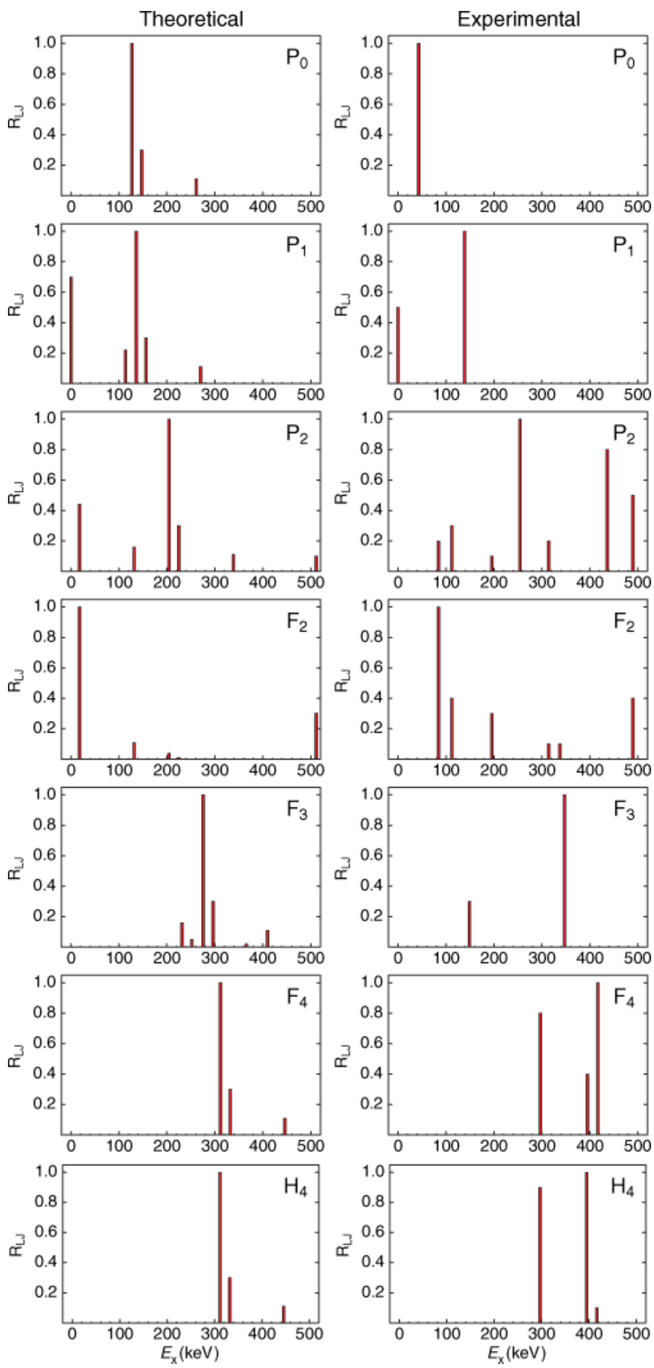

FIG. 5. (Color online) Comparison of theoretical and experimental values of ratios R_{LJ} of spectroscopic strengths (cf. Table VIII).

V. CONCLUSIONS

An essentially extended level scheme including 60 levels is proposed for the odd-odd nucleus ^{194}Ir. The γ decay and spin-parity assignments are given. The scheme is discussed in comparison with the axially symmetric prolate model and the extended supersymmetry. For a number of bandheads, appropriate rotational levels are proposed. If one does not expect exact rotational energy relations of the type $I(I+1)$, a search for rotational bands can be justified. Other approaches within geometric models are possible. Probably, triaxiality could be used, because it was already tested for several odd iridium nuclei [40]. We are not aware of serious studies of this kind for odd-odd nuclei. Evidently, ^{194}Ir has a small deformation.

The negative parity states of ^{194}Ir were calculated using the $U_\nu(6/12) \otimes U_\pi(6/4)$ supersymmetry. The new experimental information for ^{194}Ir, especially from the two-nucleon transfer reaction $(\vec{d}, \alpha)$, was crucial to making several changes in the assignments of quantum numbers with respect to previous studies. In addition, several new negative parity states were found. The spectroscopic properties of ^{194}Ir are in remarkable agreement with the SUSY predictions, both for energies and spectroscopic factors for two-nucleon transfer reactions. The interpretation of the experimental data on ^{194}Ir in nuclear SUSY is at least of the same quality as that for ^{196}Au [5,22,35,36,41], thus providing additional evidence for the existence of nuclear supersymmetry in the $A \sim 190$ mass region. The available spectroscopic information for the ^{192,193}Os and ^{193,194}Ir quartet of nuclei is more limited than for the Pt-Au case, especially with respect to the odd-neutron nucleus ^{193}Os. It would be very interesting to see to what extent this nucleus can be described by U(6/12). For the Pt-Au nuclei, the detailed knowledge of the odd-neutron nucleus ^{195}Pt made it possible to predict with confidence the properties of the odd-odd nucleus ^{196}Au [34]. For the Os-Ir nuclei, the properties of the ^{192}Os, ^{193}Ir, and ^{194}Ir nuclei can be used to predict those of the odd-neutron nucleus ^{193}Os, since these four nuclei are linked by supersymmetry. More details about the new classification will be published in Ref. [42].

Although the number of atomic nuclei to which the concept of supersymmetry can be applied is limited, many examples of supersymmetry have been found in atomic nuclei. Nuclear SUSY provides a set of closed expressions for energies and selection rules for electromagnetic transitions and transfer reactions which may be used as benchmarks to study and interpret the experimental data, even if these symmetries may be valid only in an approximate way. In this respect, it is a challenge for future experimental and theoretical work to continue searching for new examples of supersymmetry in nuclear physics.

ACKNOWLEDGMENTS

The authors acknowledge financial support from the Maier-Leibnitz-Labor, the Deutsche Forschungsgemeinschaft (Grant Nos. IIC4-Gr894/2-3 and JO391/2-3), from CONACyT, Mexico, and from the Science Council of Latvia (Grant No. 05.17.24).

APPENDIX

Figure 6 shows all angular distributions of the $(\vec{d}, \alpha)$ measurement at $E_x = 18$ MeV.

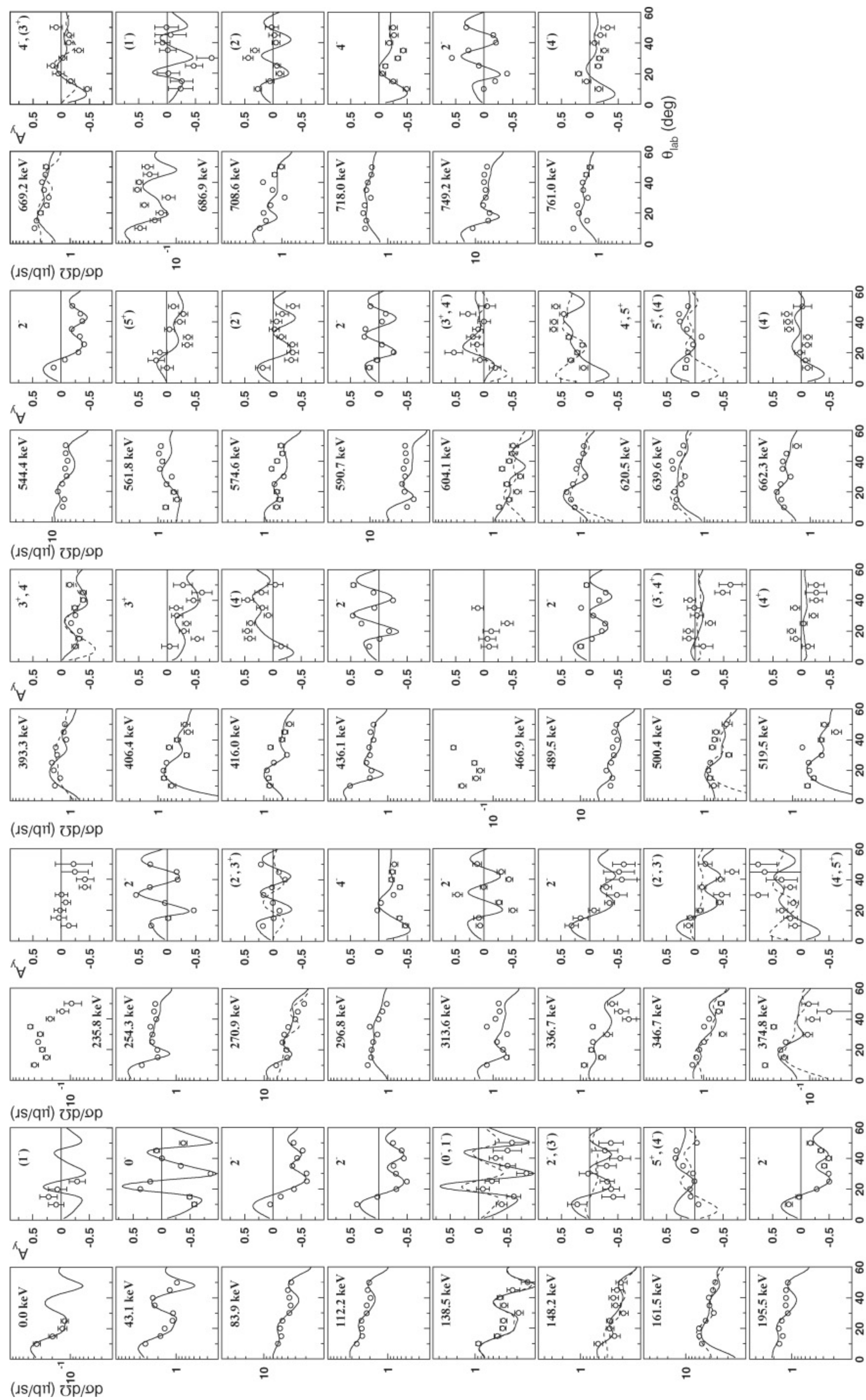

FIG. 6. All angular distributions of the ^{196}Pt$(\vec{d},\alpha)^{194}$Ir measurement at $E_x = 18$ MeV.

[1] M. Balodis, P. Prokofjevs, N. Krāmere, L. Simonova, J. Bērziņš, T. Krasta, J. Kern, A. Raemy, J. C. Dousse, W. Schwitz, J. A. Cizewski, G. G. Colvin, H. G. Boerner, P. Geltenbort, F. Hoyler, S. A. Kerr, K. Schreckenbach, R. Georgii, T. von Egidy, J. Klora, H. Lindner, U. Mayerhofer, A. Walter, A. V. Murzin, V. A. Libman, I. A. Kondurov, Yu. E. Loginov, P. A. Sushkov, S. Brant, V. Paar, and V. Lopac, Nucl. Phys. **A641**, 133 (1998).
[2] P. E. Garrett, D. G. Burke, Tao Qu, V. Paar, and S. Brant, Nucl. Phys. **A579**, 103 (1994).
[3] B. Singh, Nucl. Data Sheets **107**, 1531 (2006).
[4] J. Jolie and P. Garrett, Nucl. Phys. **A596**, 234 (1996).
[5] J. Barea, R. Bijker, and A. Frank, Phys. Rev. Lett. **94**, 152501 (2005).
[6] W. Assmann, J. de Boer, U. Meyer-Berkout, S. Skorka, E. Huenges, P. Kienle, H. Morinaga, E. Nolte, H. Münzer, L. Rohrer, and H. Schnitter, Nucl. Instrum. Methods **122**, 191 (1974).
[7] M. Löffler, H. J. Scheerer, and H. Vonach, Nucl. Instrum. Methods **111**, 1 (1973).
[8] H.-F. Wirth, H. Angerer, T. von Egidy, Y. Eisermann, G. Graw, and R. Hertenberger, Beschleunigerlaboratorium München Annual Report, 2000, p. 71, see http://www.bl.physik.uni-muenchen.de/bl_rep/jb2000/p71.ps.
[9] H.-F. Wirth, Ph.D. thesis, Technische Universität München, 2001; see http://tumb1.biblio.tu-muenchen.de/publ/diss/ph/2001/wirth.html.
[10] R. Hertenberger, A. Metz, Y. Eisermann, K. El Abiary, A. Ludewig, C. Pertl, S. Trieb, H.-F. Wirth, P. Schiemenz, and G. Graw, Nucl. Instrum. Methods Phys. Res. A **536**, 266 (2005).
[11] M. Balodis, P. Prokofjevs, N. Krāmere, L. Simonova, J. Bērziņš, T. Krasta, R. Georgii, T. von Egidy, J. Klora, H. Lindner, U. Mayerhofer, A. Walter, J. A. Cizewski, G. G. Colvin, H. G. Boerner, P. Geltenbort, F. Hoyler, S. A. Kerr, K. Schreckenbach, A. Raemy, J. C. Dousse, J. Kern, W. Schwitz, I. A. Kondurov, Yu. E. Loginov, P. A. Sushkov, S. Brant, V. Paar, and V. Lopac, Fizika (Zagreb) B **7**, 15 (1998).
[12] P. D. Kunz, computer code CHUCK3, University of Colorado; see http://spot.colorado.edu/∼kunz.
[13] MINUIT fitting routine; see http://seal.web.cern.ch/seal/work-packages/mathlibs/minuit/home.html.
[14] W. W. Daehnick, J. D. Childs, and Z. Vrcelj, Phys. Rev. C **21**, 2253 (1980).
[15] E. R. Crosson, E. J. Ludwig, M. Bisenberger, R. Hertenberger, D. Hofer, H. Kader, P. Schiemenz, G. Graw, A. M. Eiro, F. D. Santos, and B. A. Brown, Phys. Rev. C **48**, 1770 (1993).
[16] F. Merz, H. Clement, F. J. Eckle, G. Eckle, A. M. Eiro, G. Graw, H. Kader, S. Roman, P. Schiemenz, and N. Seichert, Phys. Lett. **B183**, 144 (1987).
[17] F. Merz, A. M. Eiro, F. J. Eckle, G. Eckle, G. Graw, R. Hertenberger, H. Kader, and P. Schiemenz, Nucl. Phys. **A489**, 399 (1988).
[18] G. G. Colvin, J. A. Cizewski, H. G. Börner, P. Geltenbort, F. Hoyler, S. A. Kerr, and K. Schreckenbach, ILL Grenoble report N 86Co09T, 1986 (unpublished).
[19] G. G. Colvin, H. G. Boerner, P. Geltenbort, F. Hoyler, S. A. Kerr, K. Schreckenbach, and J. A. Cizewski, Nucl. Phys. **A465**, 240 (1987).
[20] J. Kern, A. Raemy, W. Beer, J. Cl. Dousse, W. Schwitz, M. K. Balodis, P. T. Prokofjev, N. D. Kramer, L. I. Simonova, R. W. Hoff, D. G. Gardner, M. A. Gardner, R. F. Casten, R. L. Gill, R. Eder, T. von Egidy, E. Hagn, P. Hungerford, H. J. Scheerer, H. H. Schmidt, E. Zech, A. Chalupka, A. V. Murzin, V. A. Libman, I. V. Kononenko, C. Coceva, P. Giacobbe, I. A. Kondurov, Yu. E. Loginov, and P. A. Sushkov, Nucl. Phys. **A534**, 77 (1991).
[21] T. von Egidy, W. Kaiser, W. Mampe, C. Hillenbrand, W. Stöffl, R. G. Lanier, K. Mühlbauer, O. W. B. Schult, H. R. Koch, H. A. Baader, R. L. Mlekodaj, R. K. Sheline, E. B. Shera, J. Ungrin, P. T. Prokofjev, L. I. Simonova, M. K. Balodis, H. Seyfarth, B. Kardon, W. Delang, P. Göttel, D. Breitig, W. R. Kane, R. F. Casten, H. J. Scheerer, P. Glässl, E. Huenges, M. Löffler, H. Rösler, and H. K. Vonach, Z. Phys. A **286**, 341 (1978).
[22] A. Metz, J. Jolie, G. Graw, R. Hertenberger, J. Gröger, C. Günther, N. Warr, and Y. Eisermann, Phys. Rev. Lett. **83**, 1542 (1999).
[23] K. Schreckenbach, Program LEVFIT, ILL, Grenoble (unpublished).
[24] A. Lundan and A. Siivola, Nucl. Phys. **A106**, 417 (1967).
[25] A. W. Sunyar, G. Scharff-Goldhaber, and M. McKeown, Phys. Rev. Lett. **21**, 237 and 506 (1968).
[26] F. Iachello, Phys. Rev. Lett. **44**, 772 (1980).
[27] F. Iachello and A. Arima, *The Interacting Boson Model* (Cambridge University, Cambridge, England, 1987).
[28] F. Iachello and O. Scholten, Phys. Rev. Lett. **43**, 679 (1979).
[29] F. Iachello and P. Van Isacker, *The Interacting Boson-Fermion Model* (Cambridge University, Cambridge, England, 1991).
[30] A. B. Balantekin, I. Bars, and F. Iachello, Phys. Rev. Lett. **47**, 19 (1981); Nucl. Phys. **A370**, 284 (1981).
[31] R. Bijker, Ph.D. thesis, University of Groningen, 1984.
[32] J. A. Cizewski, R. F. Casten, G. J. Smith, M. L. Stelts, W. R. Kane, H. G. Börner, and W. F. Davidson, Phys. Rev. Lett. **40**, 167 (1978); A. Arima and F. Iachello, Phys. Rev. Lett. **40**, 385 (1978).
[33] A. B. Balantekin, I. Bars, R. Bijker, and F. Iachello, Phys. Rev. C **27**, 1761 (1983).
[34] P. Van Isacker, J. Jolie, K. Heyde, and A. Frank, Phys. Rev. Lett. **54**, 653 (1985).
[35] J. Gröger, J. Jolie, R. Krücken, C. W. Beausang, M. Caprio, R. F. Casten, J. Cederkall, J. R. Cooper, F. Corminboeuf, L. Genilloud, G. Graw, C. Günther, M. de Huu, A. I. Levon, A. Metz, J. R. Novak, N. Warr, and T. Wendel, Phys. Rev. C **62**, 064304 (2000).
[36] H.-F. Wirth, G. Graw, S. Christen, Y. Eisermann, A. Gollwitzer, R. Hertenberger, J. Jolie, A. Metz, O. Möller, D. Tonev, and B. D. Valnion, Phys. Rev. C **70**, 014610 (2004).
[37] M. Vergnes, in *Nuclear Structure, Reactions and Symmetries*, edited by R. A. Meyer and V. Paar (World Scientific, Singapore, 1986), p. 187.
[38] J. A. Cizewski, D. G. Burke, E. R. Flynn, R. E. Brown, and J. W. Sunier, Phys. Rev. C **27**, 1040 (1983).
[39] R. Bijker and O. Scholten, Phys. Rev. C **32**, 591 (1985).
[40] S. E. Drissi, Nucl. Phys. **A621**, 655 (1997).
[41] J. Barea, R. Bijker, and A. Frank, J. Phys. A: Math. Gen. **37**, 10251 (2004).
[42] J. Barea *et al.* (work in progress).